

# Effect of Addition of Palm Oil Biodiesel in Waste Plastic Oil on Diesel Engine Performance, Emission, and Lubricity

Muhamad Sharul Nizam Awang,\* Nurin Wahidah Mohd Zulkifli,\* Muhammad Mujtaba Abbas, Syahir Amzar Zulkifli, Md Abul Kalam, Muhammad Hazwan Ahmad, Mohd Nur Ashraf Mohd Yusoff, Mazrina Mazlan, and Wan Mohd Ashri Wan Daud



Cite This: *ACS Omega* 2021, 6, 21655–21675



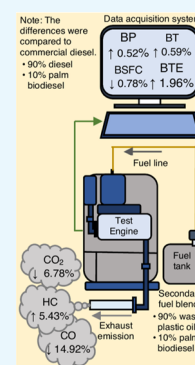
Read Online

ACCESS |

Metrics & More

Article Recommendations

**ABSTRACT:** This research was aimed to examine the diesel engine's performance and emission of secondary fuels (SFs), comprising waste plastic oil (WPO) and palm oil biodiesel (POB), and to analyze their tribological properties. Their compositions were analyzed by gas chromatography–mass spectrometry (GC–MS). Five SFs (10–50% POB in WPO) were prepared by mechanical stirring. The results were compared to blank WPO (WPO100) and Malaysian commercial diesel (B10). WPO90 showed the maximum brake power (BP) and brake torque (BT) among the SFs, and their values were 0.52 and 0.59% higher compared to B10, respectively. The increase in POB ratio (20–50%) showed a negligible difference in BP and BT. WPO70 showed the lowest brake-specific fuel consumption among the SFs. The brake thermal efficiency (BTE) increased with POB composition. The maximum reductions in emission of hydrocarbon (HC, 37.21%) and carbon monoxide (CO, 27.10%) were achieved by WPO50 among the SFs. WPO90 showed the maximum reduction in CO<sub>2</sub> emission (6.78%). Increasing the POB composition reduced the CO emissions and increased the CO<sub>2</sub> emissions. All SFs showed a higher coefficient of friction (COF) than WPO100. WPO50 showed the minimal increase in COF of 2.45%. WPO90 showed the maximum reduction in wear scar diameter (WSD), by 10.34%, compared to B10. Among the secondary contaminated samples, SAE40-WPO90 showed the lowest COF, with 5.98% reduction compared to SAE40-WPO100. However, with increasing POB content in the secondary contaminated samples, the COF increased. The same trend was also observed in their WSD. Overall, WPO90 is the optimal SF with excellent potential for diesel engines.



## 1. INTRODUCTION

Since the start of the industrial age, the global energy consumption has been growing continuously, corresponding to mankind needs. Because the world population is increasing and emerging nations' economies are growing fast, energy consumption is not projected to decline in this century. The primary energy sources such as coal, oil, and natural gas, on the other hand, appear to be reaching a critical point.<sup>1</sup> The petroleum fuels are presently the primary source of carbon dioxide (CO<sub>2</sub>) emissions, greenhouse gases, and global warming. Exploring sustainable alternatives to conventional petroleum fuels has become necessary due to the depletion of petroleum supplies and an increase in environmental pollution. The vehicle population, industrialization, increased domestic economic load, rising energy consumption, population growth, pollution, and other factors all point to the need for alternate fuels.<sup>2</sup>

Due to its superior characteristics (cetane number, oxygen (O<sub>2</sub>) content, etc.) over diesel, biodiesel exhibits a significant reduction in several key exhaust pollutants such as carbon monoxide (CO) and hydrocarbons (HC). Palm oil biodiesel (POB) is the most significant biofuel due to its enhanced properties compared to other biodiesels: larger contribution (35%), lower price (\$660 USD/ton), higher oil content (5000

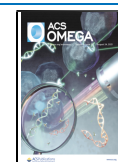
kg oil/ha), and better production output (4.2 MT/ha).<sup>3</sup> Palm oil is the major raw material for the manufacturing of biodiesel in Malaysia, as it is the country's main agricultural export commodity. As a result, Malaysia has upped its current biodiesel requirements to B10 (10% for POB and 90% for diesel) in order to assist the palm oil sector.<sup>4</sup>

The yearly plastic trash created in the world and in Malaysia is shown in Figure 1. In 2018, the global output of plastic trash was estimated to be at 359 million tonnes, up by 3% from 2017. Malaysia produced about 1.83 million tonnes in 2018. In comparison to 2018, the volume of plastic trash in Malaysia would rise to 2.09 million tonnes by 2025.<sup>5</sup> Due to a lack of knowledge about the rising pollution caused by plastics in modern life, the public continues to engage in environmentally irresponsible dumping. Although there are a variety of regulations in place to regulate waste, one typical method is to collect solid waste from individual houses and then dispose

Received: June 10, 2021

Accepted: July 30, 2021

Published: August 13, 2021



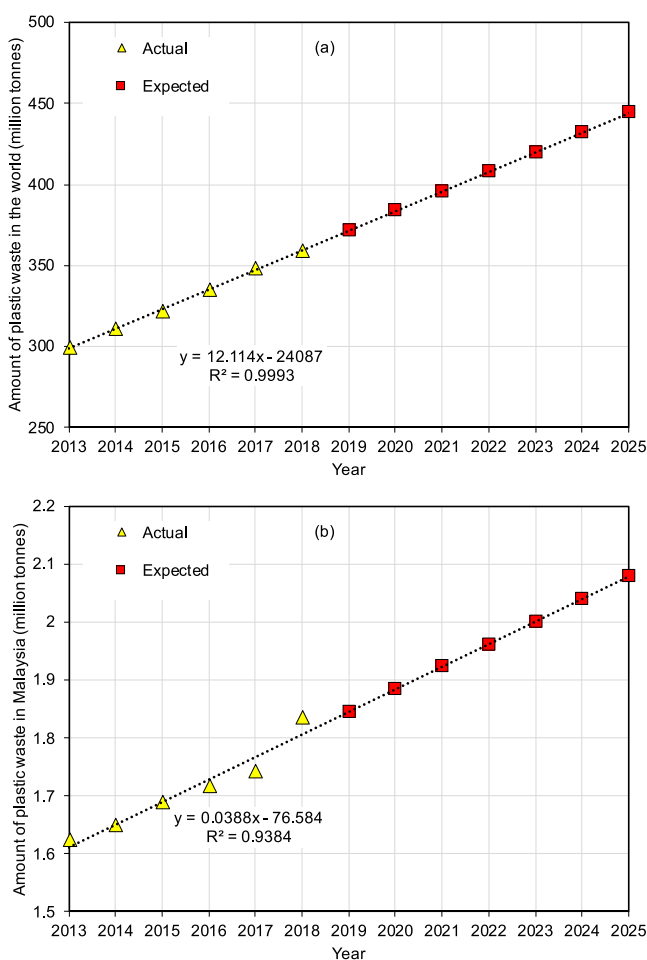


**Figure 1.** Generation of plastic waste in (a) the world and (b) Malaysia.<sup>15</sup>

it off in a landfill. As a result, land pollution, water contamination, and environmental contamination occur. The researchers are highly concerned about pyrolysis of plastic waste to relieve pollution and energy catastrophes, since plastic garbage is abundant and can be utilized effectively as energy.

In terms of viscosity, flash point, density, and calorific value, waste plastic oil (WPO) is similar to diesel.<sup>6</sup> As a result, WPO has been investigated in terms of engine performance, with no major changes found compared to diesel.<sup>7</sup> Although the resultant WPO has a lower viscosity (2.9 cSt) than diesel (3.1 cSt), it aids in the production of tiny droplets during atomization, allowing for sufficient combustion.<sup>8</sup> As a result, WPO contributes to improvement of the BSFC.<sup>8</sup> WPO's BTE was likewise around 5% greater than that of diesel.<sup>7,9</sup> In fact, WPO is becoming one of the most popular alternative fuels owing to its ability to increase the performance of diesel engines.

However, WPO (38.3–44.9 MJ/kg) has a lower calorific value than diesel (42.0–45.6 MJ/kg), according to most research.<sup>8,10–14</sup> The low calorific value of WPO was partly attributable to the rise of the BSFC by 11.1, 3.0, and 5.7% compared to diesel, according to Kalargaris et al.,<sup>10</sup> Khatha et al.,<sup>12</sup> and Kumar et al.,<sup>13</sup> respectively. Furthermore, Kalargaris et al.<sup>10</sup> and Mangesh et al.<sup>11</sup> found that the low calorific value of WPO reduced the BTE when compared to diesel. The poor heating value of WPO also results in 33.7% greater CO emissions as compared to diesel.<sup>13</sup> According to Kalargaris et

al.,<sup>10</sup> WPO contains a significant amount of aromatics, which lowers the BTE by 5.7% when compared to diesel. When compared to diesel, Kumar et al.<sup>13</sup> and Kalargaris et al.<sup>10</sup> found that a significant quantity of aromatics in WPO also reduced HC emissions by 43.8 and 85.1%, respectively. WPO application increases emissions from diesel engines and may impair diesel engine performance in general; therefore, researchers should be mindful of this.

It has been claimed that utilizing WPO and biodiesel mixes in diesel engines might become an alternative method to achieve cleaner fuel combustion that leads to improvements, taking into account the emissions caused by the presence of O<sub>2</sub> in the fuel molecules. Kaewbuddee et al.<sup>7</sup> investigated the use of WPO in combination with biodiesel (POB) or castor oil biodiesel (COB) as an alternative fuel for diesel engines and discovered that adding 10% of each to WPO increased the BTE by 2.07% and the BSFC by 1.27 and 1.66%, respectively, when compared to blank WPO. These mixtures also reduced the HC and NO<sub>x</sub> emission by up to 3.45 and 8.21%, respectively, while CO emission increased by 8.47% (POB–WPO mixture) and 15.33% (COB–WPO mixture) compared to pure WPO. Ramesha et al.<sup>16</sup> reported that B20 algae biodiesel mixed with WPO can be a suitable fuel for diesel engines. When compared to pure diesel, the BTE of the WPO–biodiesel combination increased by 12.36%. In addition, as compared to pure diesel, HC and CO emissions were reduced, although NO<sub>x</sub> increased somewhat. WPO was combined with 10 and 20% Jatropa biodiesel (JB) for diesel engines in the research by Senthilkumar and Sankaranarayanan.<sup>17</sup> For both mixes, the BTE and BSFC were approximately 9 and 6% higher than that of WPO, respectively, whereas HC and CO emissions dropped.

The fuel pump and fuel injector, for example, are self-lubricating diesel engine components. Lubricity, in fact, is critical for improving the overall efficiency of engine components.<sup>18,19</sup> Using the high-frequency reciprocating rig (HFRR) based on the ASTM D6079 standard, Awang et al.<sup>20</sup> evaluated the lubricity of the WPO and reported the lowest coefficient of friction (COF). WPO can be mixed with biodiesel to increase the lubricity, according to Kaewbuddee et al.<sup>7</sup> When compared to blank WPO, they found that adding 10% POB and up to 15% COB to the WPO reduced the wear scar diameter (WSD) by 1.10 and 2.62%, respectively.

In fact, WPO has the potential to be a source of fuel for the automobile sector. For future prospects, because use of WPO alone is not desirable owing to its physicochemical characteristics, WPO will be combined with POB because of its benefits and high O<sub>2</sub> content in the fuel molecules. There are just a few studies on diesel engine testing for WPO–biodiesel fuel blends, according to the literature review, and the bulk of them only use up to 20% of biodiesel. Therefore, up to 50% of POB was combined with WPO to produce secondary blends for diesel engine usage in this experiment to examine the effect of the increasing biodiesel content in WPO on its performance, emission, and lubricity. Only one research on the tribological effects of WPO–POB fuel blends was published, and it only provided the average change in WSD, which is insufficient to explain the lubricity effects of these blends. As a result, the impact of the percentage of POB in WPO on the tribological characteristics of diesel engine components was thoroughly examined in this study, in terms of COF during the run-in and steady-state periods, average COF, and WSD. This study also focused at the lubrication degradation caused by dilution using

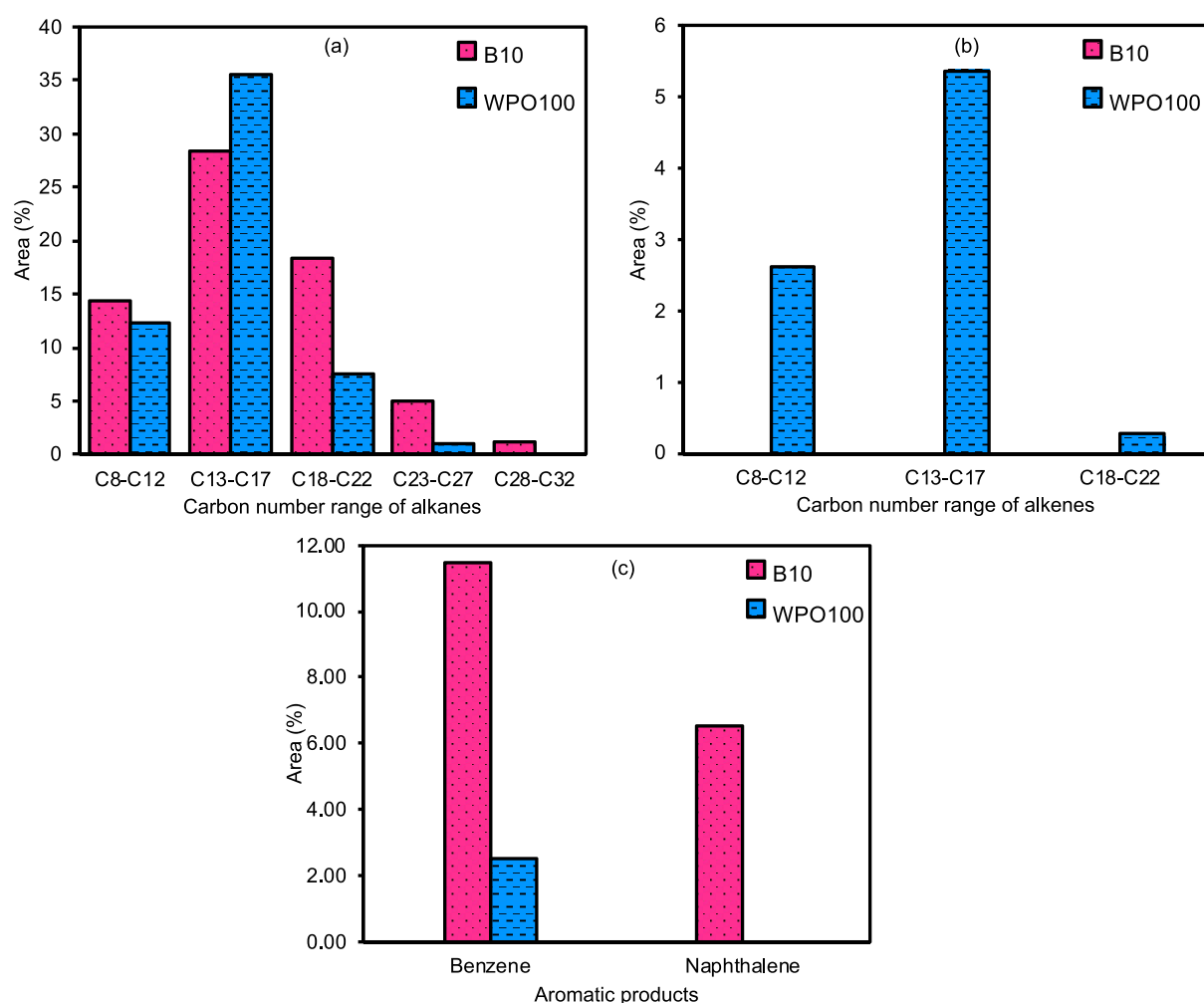


**Figure 2.** Carbon number ranges of (a) alkane and (b) alkene products, and (c) composition of the aromatic products of B10 and WPO100.

WPO-POB mixes, which has never been done previously. After that, the effects of blending up to 50% POB in WPO to produce secondary fuels (SFs) on diesel engine performance (brake power (BP), brake torque (BT), BTE, and BSFC), emissions (HC, CO, and CO<sub>2</sub>), and lubricity were thoroughly investigated and compared to Malaysian commercial diesel (B10) and blank WPO fuel (WPO100). The effects of SFs on the lubricity and tribological characteristics of commercial lubricants were also studied in depth.

## 2. RESULTS AND DISCUSSION

**2.1. Gas Chromatography–Mass Spectrometry (GC–MS) Analysis.** Figure 2 shows the carbon number range of the alkane and alkene products, and the composition of the aromatic products of B10 and WPO100. Figure 2 shows that most of the chemical components in B10 are alkanes. The B10 contains approximately 67.17, 11.49, and 6.54% of alkanes, benzene, and naphthalene, respectively, and no alkenes are detected in B10. Mangesh et al.<sup>11</sup> also reported the same results that diesel contains 50.00, 28.81, and 13.73% of alkanes, benzene, and naphthalene, respectively. The GC–MS data of WPO100 shows the presence of 60.70, 8.29, and 2.52% of alkanes, alkenes, and benzene, respectively, and the absence of naphthalene. Mangesh et al.<sup>11</sup> also observed the same trend that WPO100 shows the presence of alkenes but diesel comparatively shows only traces of alkenes. Alkene compounds

contain unsaturated double bonds, which cause a high rate of heat release during combustion in diesel engines.<sup>11</sup>

Figure 2a shows that the GC–MS data are ordered according to the number of carbon atoms of the alkane compounds present in B10 and WPO100. B10 contains 14.37 and 52.80% of the C<sub>8</sub>–C<sub>12</sub> and C<sub>13</sub>–C<sub>32</sub> ranges of alkanes, respectively. WPO100 also shows the same trends as B10 that most of the alkanes are in the range of C<sub>13</sub>–C<sub>32</sub> (44.11%) and C<sub>8</sub>–C<sub>12</sub> (12.38%). The study also shows that the alkane content of WPO in the range of C<sub>13</sub>–C<sub>32</sub> is 16.46% lower than that of B10. This could be the reason why the viscosity of WPO100 is lower than that of B10, as shown in Table 6, and is therefore suitable for diesel injection in diesel engines.<sup>11</sup> Figure 2b shows the GC–MS data, which are arranged according to the carbon number range of the alkene compounds present in WPO100. WPO100 contains heavier HC (C<sub>13</sub>–C<sub>32</sub>) (5.66%) than the gasoline fraction content (C<sub>8</sub>–C<sub>12</sub>) (2.63%). Figure 2c shows the GC–MS data for the aromatic compounds present in B10 and WPO100. The latter contains 2.52% of aromatic compounds, which is lower than that in the literature (39%).<sup>21</sup> Compared with B10, WPO100 has 78.07% lower benzene content without the presence of naphthalene. As WPO100 contains fewer aromatic compounds than B10, it can only be used as a mixed fuel with diesel.

The chemical compositions of POB, WCOB, and B10 are shown in Table 1. Oleic acid has the highest level of fatty acid

Table 1. Chemical Compositions of POB, WCOB, and B10

fatty acid			area (%)	
common name	IUPAC name	structure	POB	B10
caprylic acid	octanoic acid	C8:0	0.34	
capric acid	decanoic acid	C10:0	0.10	
lauric acid	dodecanoic acid	C12:0	1.28	
myristic acid	tetradecanoic acid	C14:0	4.79	
pentadecanoic acid	pentadecanoic acid	C15:0	0.29	
palmitic acid	hexadecanoic acid	C16:0	34.74	3.83
heptadecanoic acid	heptadecanoic acid	C17:0	0.58	
oleic acid	<i>cis</i> -9-octadecenoic acid	C18:1	48.45	
linoleic acid	<i>cis</i> -9,12-octadecatrienoic acid	C19:2		4.39
arachidic acid	eicosanoic acid	C20:0		0.38
gondoic acid	<i>cis</i> -11 eicosenoic acid	C20:1	1.07	
lignoceric acid	tetracosanoic acid	C24:0	1.23	
total saturated fatty acids			43.35	4.21
total unsaturated fatty acids			49.52	4.39

methyl esters (FAME) in POB (48.5%), followed by palmitic acid (34.7%). Ali et al.<sup>22</sup> (oleic acid (49.2%) and palmitic acid (43.3%)), Razzaq et al.<sup>23</sup> (oleic acid (45.0%) and palmitic acid (39.9%)), and Kaewbuddee et al.<sup>7</sup> (oleic acid (37.07%) and palmitic acid (46.29%)) also observed the same results. In general, the unsaturated fatty acids dominate the POB composition (49.5%). Razzaq et al.<sup>23</sup> reported the same observation. However, this result does not agree with the result of Ali et al.,<sup>22</sup> which reported that the highest component of POB is saturated fatty acids (50.6%). B10 contains 10% POB and 90% petroleum diesel,<sup>4</sup> so its FAME content is lower than that of pure POB. Table 1 shows that B10 contains the highest level of linoleic acid (3.83%), followed by palmitic acid (3.83%). In the composition of B10, unsaturated fatty acids are also the main component (4.39%). Table 2 shows the carbon

Table 2. Carbon Length Distribution of Saturated and Unsaturated Fatty Acids in POB and B10<sup>a</sup>

length of carbon	POB		B10	
	SFA (%)	USFA (%)	SFA (%)	USFA (%)
SCFA (C1–C5)	NP	NP	NP	NP
MCFA (C6–C12)	1.72	NP	NP	NP
LCFA (C13–C21)	40.4	49.52	3.32	NP
VLCFA (C22 and above)	1.23	NP	NP	NP

<sup>a</sup>SFA = saturated fatty acid, USFA = unsaturated fatty acid, SCFA = short-chain fatty acid, MCFA = medium-chain fatty acid, LCFA = long-chain fatty acid, VLCFA = very-long-chain fatty acid, NP = not present.

length distribution of saturated and unsaturated fatty acids contained in POB and B10 from the previous studies. Most of the fatty acids contained in POB are long-chain fatty acids (LCFA), which can lead to an incomplete combustion.<sup>24</sup> The HC and CO emissions can increase as the length of the fatty acid chain increases. This trend can be explained by the lower O<sub>2</sub> content in the longer fatty acid molecules, which leads to an incomplete combustion. In addition, fatty acids with longer chain lengths have higher boiling and melting points, making them unlikely to be completely vaporized and burned, thereby increasing HC and CO emissions.<sup>25</sup>

## 2.2. Engine Performance. 2.2.1. Engine Brake Power.

Figure 3a shows the engine BP of all samples as a function of engine speed at 100% engine load. A significant variation in BP of each fuel at the entire speeds is observed. It is clear that the BPs of all samples show escalating trends with respect to the rise in engine speed. For B10, WPO90, WPO80, WPO60, WPO50, WPO70, and WPO100, the maximum power values obtained at 2400 rpm are 7.41, 7.38, 7.03, 6.97, 6.93, 6.89, and 6.82 kW, respectively. In all engine speed ranges (900–2400 rpm), the average BPs of WPO90, B10, WPO60, WPO50, WPO80, WPO100, and WPO70 are 5.50, 5.47, 6.97, 5.36, 5.34, 5.34, and 5.33 kW, respectively. Figure 3b shows the average BP value and the change in BP compared to B10 and WPO100. The average BP of WPO90 increased slightly by 0.52% compared to B10. This result agrees well with the study by Monirul et al.,<sup>26</sup> who reported a 4.19% increase in BP when 10% POB was added to diesel compared to pure diesel. This is due to the increase in O<sub>2</sub> content, in the fuel molecule of the fatty acid in POB, resulting in a more effective combustion.<sup>7,27</sup> In addition, the lower density and viscosity of B10 can influence the power loss due to higher leakages at the fuel pump compared with WPO100.<sup>26</sup> Meanwhile, Ali et al.<sup>22</sup> reported a decrease of 0.49% in BP by adding 10% POB to diesel compared to pure diesel. However, increasing the POB composition up to 20% in the SFs decreased the BP.

The average BP of WPO60, WPO50, WPO80, WPO70, and WPO100 decreased by 1.60, 2.03, 2.43, 2.43, and 2.44%, respectively, compared to B10. As shown in Table 6, the decrease in BP is attributed to their lower heating value and higher viscosity than that of B10,<sup>28,29</sup> dominated by the increase of O<sub>2</sub> content in the blends. WPO has a high energy density because it consists of hydrogen and carbon. However, the low calorific value of POB (39.98 MJ/kg) dominates the high calorific value of WPO (45.61 MJ/kg). These results agree with the study by Ali et al.,<sup>22</sup> in which BP was lowered by 2.58% by adding up to 30% POB to diesel compared to pure diesel. As a result of this, poor atomization and uneven combustion occurred, which led to a decrease in BP.<sup>29</sup> Compared with WPO100, the BP average of SF mixtures (WPO90, WPO60, WPO50, WPO70, and WPO80) increased by 3.03, 0.85, 0.42, 0.01, and 0.01%, respectively. The relatively high BP of the quaternary mixture can be related to the higher O<sub>2</sub> content in the shorter fatty acid molecules of the WCOB, which dominates the lower calorific value and leads to a better evaporation and combustion.<sup>29,30</sup> The ignition delay time is increased in the case of SF mixtures, which resulted in a better combustion performance due to the lower cetane number of SF mixtures and the higher latent heat of vaporization. Similar results have been reported with the use of O<sub>2</sub>-containing alcoholic fuel additives.<sup>30,31</sup> Figure 3b also shows that WPO80 has a 2.93% reduction of BP compared to WPO90. This difference is due to the higher viscosity and lower calorific value of WPO80 compared to WPO90.<sup>22</sup> The results agree well with Ali et al.,<sup>22</sup> but Monirul et al.<sup>26</sup> reported that the addition of 20% POB to diesel fuel increased the BP value by 150.12% compared to 10% POB. An increase in the POB content in the SF blends from 20 to 50% shows a negligible difference in BP.

2.2.2. Engine Brake Torque. Figure 4a shows the engine brake torque (BT) for all fuel samples with variable engine speed at 100% engine load. All fuels tested that showed an increase in the BT value were observed at low speeds, and then a decrease was observed at medium speeds. The maximum

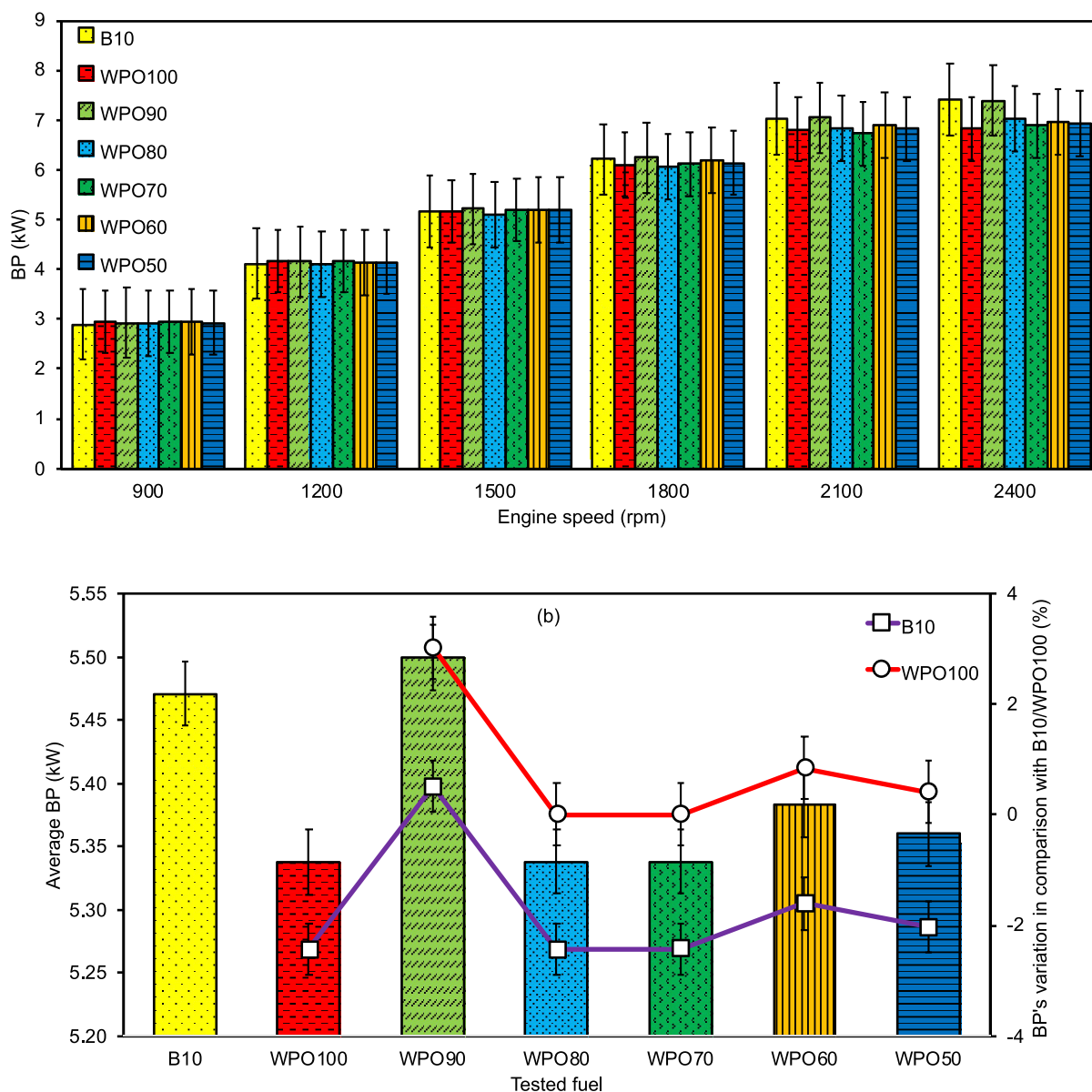


**Figure 3.** (a) Variation of BP for all tested fuels according to engine speed at full-load condition; (b) average BP and BP's variation in comparison with B10 and WPO100 for the tested fuels.

torque values for all fuels tested were 33.27, 33.27, 33.24, 33.16, 33.05, 32.50, and 33.13 Nm and were obtained at 1200 rpm for WPO100, WPO90, WPO70, WPO50, B10, WPO80, and WPO60 fuel, respectively. Figure 4b shows the average value of BT and the change in BT compared to B10 and WPO100. The average BT of all tested fuels (WPO90, B10, WPO60, WPO50, WPO100, WPO80, WPO70) was 32.06, 31.87, 31.57, 31.47, 31.39, 31.26, and 31.09 Nm, respectively. Compared to B10, the average BT value of WPO90 increased by 0.59%, while the average BT value for WPO60, WPO50, WPO100, WPO80, and WPO70 decreased slightly by 0.92, 1.23, 1.51, 1.89, and 2.44 Nm, respectively. Compared to WPO100 fuel, the BT value of WPO90, WPO60, and WPO50 fuel increased by 2.14, 0.60, and 0.29%, respectively. This is because the  $O_2$  content in POB is higher, which dominates the higher viscosity and density, leading to the phenomenon of complete combustion.<sup>22</sup> Therefore, more power will be generated, and the average pressure in the engine cylinder will be higher, resulting in an increase in BT and piston force.<sup>32</sup>

Meanwhile, the average BT value for WPO80 and WPO70 decreased slightly by 0.39 and 0.95%, respectively. Due to the lower heat generation, WPO80 and WPO70 have a lower BT value compared with WPO100. As the engine speed increased from 1200 to 2400 rpm, the average BT value of all measured fuels decreased by 115.69%. This is due to the insufficient filling of the combustion chamber during the intake stroke, and the volumetric efficiency of valve is reduced due to the complete opening of the valve, since there is not enough time for a sufficient intake phase, which leads to a reduction of the combustion chamber pressure.<sup>32,33</sup> The increase in the POB proportion in the SF mixture from 20 to 50% has a negligible influence on BT.

**2.2.3. Brake-Specific Fuel Consumption.** Figure 5a shows the BSFC results for all fuel samples under 100% load condition with variable engine speed. The BSFC of all tested fuels decreased with the increasing engine speed. The minimum BSFC values of all tested fuels (B10, WPO60, WPO50, WPO100, WPO70, WPO90, and WPO80) recorded

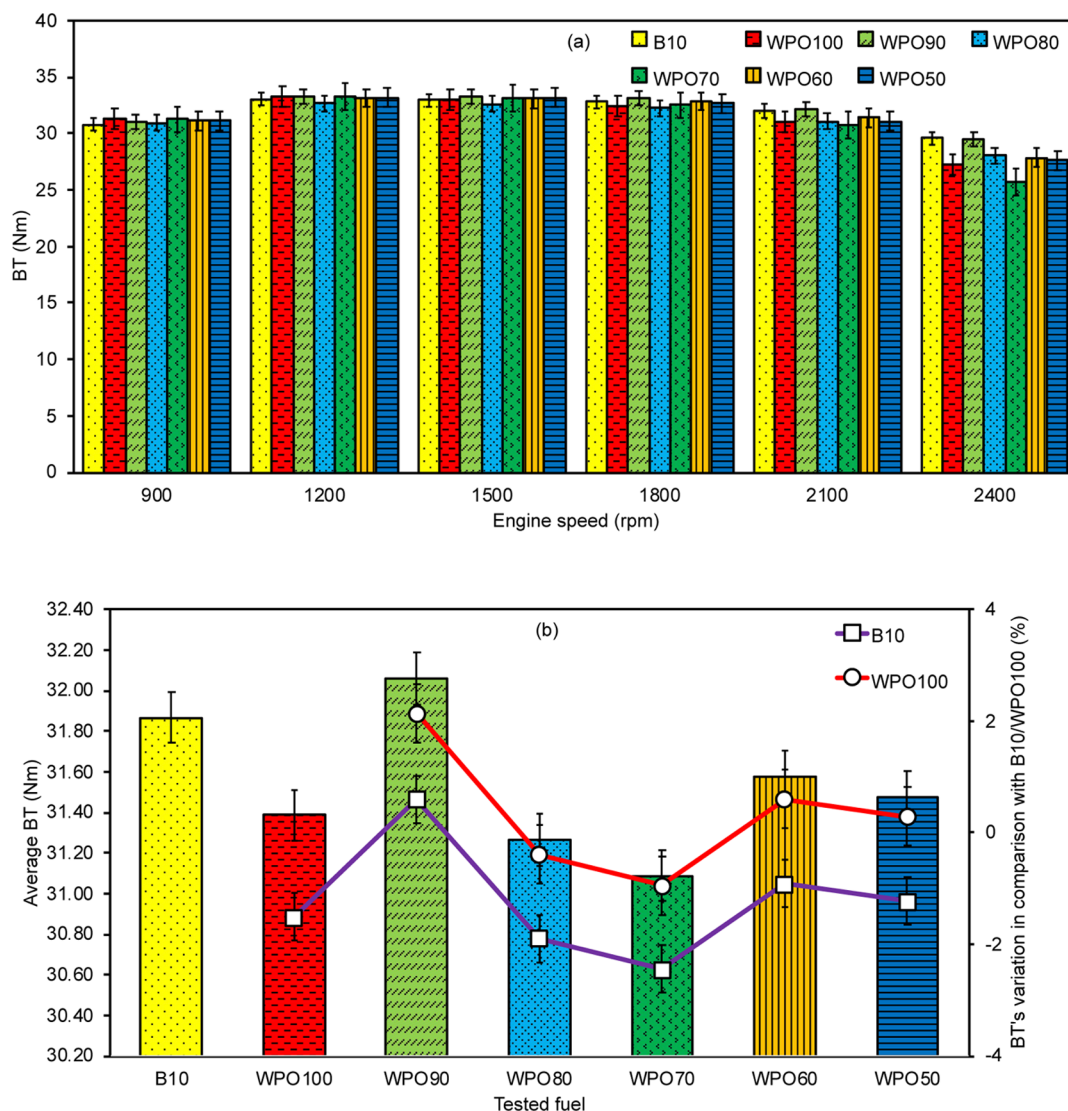


**Figure 4.** (a) Variation of BT for all tested fuels according to engine speed at full-load condition; (b) average BT and BT's variation in comparison with B10 and WPO100 for the tested fuels.

at a speed of 2400 rpm were 0.34, 0.35, 0.35, 0.36, 0.38, 0.39, and 0.42 kg/kWh, respectively. Figure 5b shows the average value of BSFC and the change in BSFC compared to B10 and WPO100. The average BSFC values of all tested fuels are 0.421 kg/kWh (WPO100), 0.438 kg/kWh (WPO70), 0.442 kg/kWh (WPO60), 0.453 kg/kWh (WPO50), 0.455 kg/kWh (WPO90), 0.458 kg/kWh (B10), and 0.475 kg/kWh (WPO80). Compared to B10, the BSFC of WPO80 is 3.61% higher, which is due to its lower calorific value, injector performance, high viscosity, and O<sub>2</sub> supply.<sup>34</sup> At the same time, the BSFC of WPO100, WPO70, WPO60, WPO50, and WPO90 decreased by 8.23, 4.42, 3.61, 1.18, and 0.78%, respectively. Compared to B10, WPO100's BSFC is 8.23% lower, which is due to the lower viscosity, dominating its lower calorific value, leading to better atomization and combustion efficiency.<sup>35</sup> The same trend (lower BSFC with lower calorific value) was also observed by Imtenan et al.<sup>35</sup>

Compared to WPO100, the average increments in BSFC for all SF mixtures (WPO80, WPO90, WPO50, WPO60, and WPO70) are 12.90, 8.12, 7.69, 5.03, and 4.15%, respectively. Mainly, increasing the BSFC of all SF blends leads to an increase in fuel consumption due to decrease in the calorific

value of the fuel in order to achieve the corresponding power output.<sup>36,37</sup> In addition, the secondary mixtures show a higher BSFC due to the higher viscosity and density values, which leads to a deteriorated air–fuel mixture and a poor atomization effect. The increase in volumetric efficiency reduces the workload during the compression stroke and thus increases the BSFC value of the SF mixture.<sup>38,39</sup> The results are in good agreement with the study by Kaewbuddee et al.<sup>7</sup> They reported that the addition of 10% POB to WPO increased the BSFC by 1.27% compared to pure WPO.

All of the secondary blends based on the volumetric efficiency required a larger fuel delivery to get the same engine power output. Higher density and lower calorific value are the main factors for this result. Higher fuel consumption can be caused by the effect of volumetric fuel injection rate at a higher viscosity of biodiesel blends.<sup>26</sup> Therefore, WPO70 displays a lower specific fuel consumption than other secondary mixtures. It is also reported by Monirul et al.<sup>26</sup> that the diesel blended with 10% calophyllum inophyllum biodiesel consumed less fuel. On the other hand, biodiesel is an O<sub>2</sub>-containing fuel and leads to a more complete combustion. Hence, BSFC is reduced. It can be seen from Figure 5b that

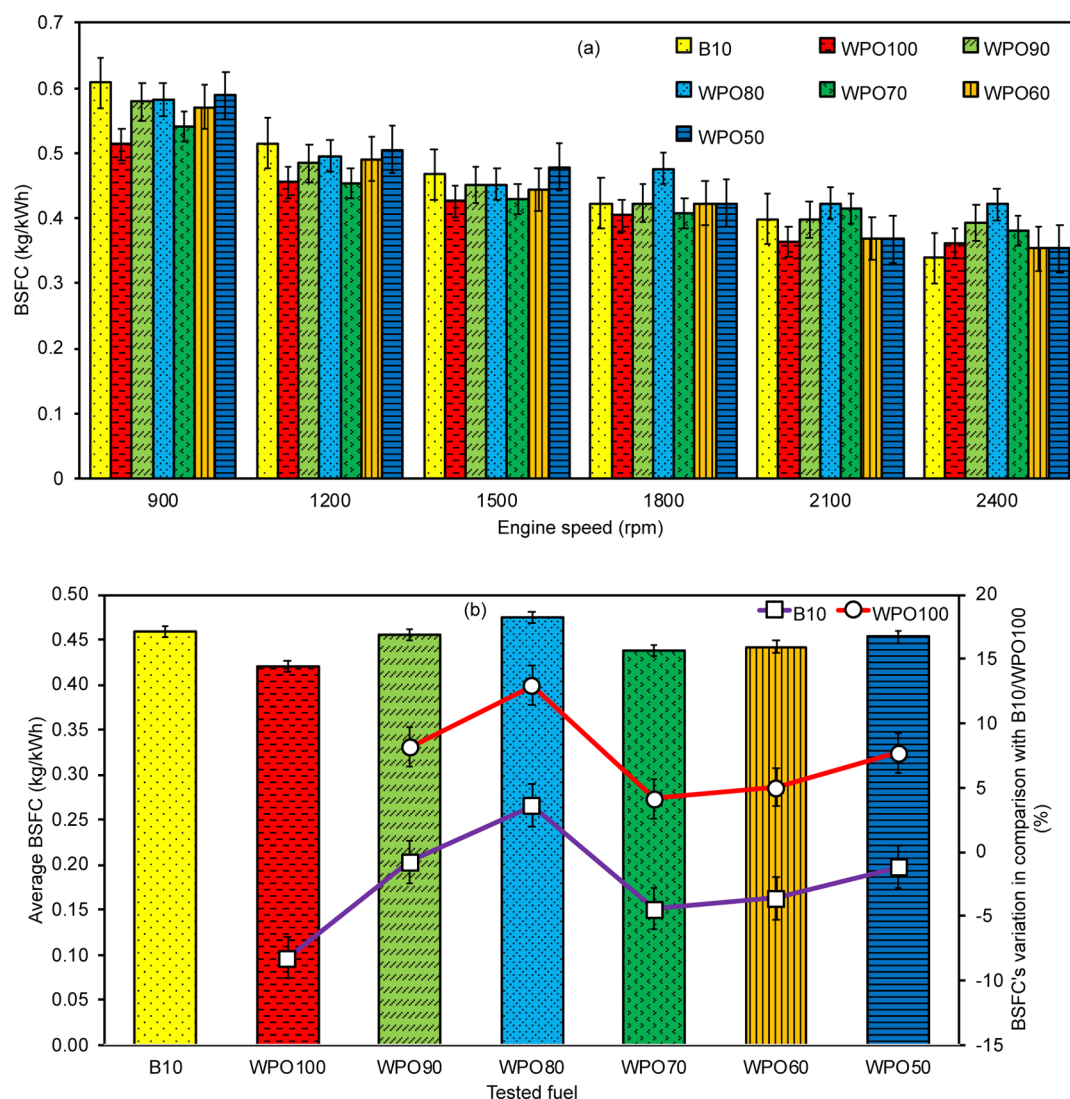


**Figure 5.** (a) Variation of BSFC for all tested fuels according to engine speed at full-load condition; (b) average BSFC and BSFC's variation in comparison with B10 and WPO100 for the tested fuels.

the  $O_2$  content is more effective than the calorific value and density in terms of lowering the BSFC for up to 30% POB content in secondary blends.

**2.2.4. Break Thermal Efficiency.** Figure 6a shows the BTE changes for all of the tested fuels under full engine load (900–2400 rpm). All tested fuels showed an increase in the BTE at 2100 rpm, and then a slight decrease in the BTE at 2400 rpm, due to a poor air–fuel mixture and spray characteristics at higher engine speed. For all tested fuels (WPO50, WPO60, WPO100, B10, WPO70, WPO90, and WPO80), the maximum BTE values obtained at 2100 rpm were recorded at 23.95, 23.99, 23.39, 23.21, 21.36, 20.55, and 20.23%, respectively. Figure 6b shows the average BTE value and BTE change compared to B10 and WPO100. The average BTE values of WPO100, WPO50, WPO60, WPO70, WPO90, WPO80, and B10 at entire engine speeds (900–2400 rpm) are 20.41, 23.95, 19.70, 18.18, 18.10, and 17.75%, respectively. Compared to B10 diesel, the BTE of WPO100, WPO50, WPO60, WPO70, WPO80, and WPO90 increased by 14.99, 11.64, 10.96, 5.82, 2.42, and 1.96%, respectively. These differences are due to the high  $O_2$  content of SFs compared to B10, which improves the fuel combustion process, and the additional lubricity provided

by the POB. These results are in agreement with earlier studies<sup>22,40</sup> that found an improvement in the BTE with increasing concentration of biodiesel in the blend with diesel. Mujtaba et al.<sup>30</sup> also reported similar results with ternary fuel.

Compared to WPO100, the BTE of all SF mixtures (WPO50, WPO60, WPO70, WPO80, and WPO90) decreased by 2.91, 3.50, 5.36, 7.97, 10.93, and 11.33%, respectively. The high viscosity and density of SFs lead to poor atomization and reduce the power and BTE. In addition, POB contains a high content of long-carbon chain fatty acids (86.07%) in the  $C_{16}$ – $C_{24}$  range. These long-chain fatty acid fractions burn late in the expansion stroke and increase the heat dissipated from the exhaust gases. At a certain power output, the fuel consumption is increased, and the BTE is reduced.<sup>41</sup> The ignition delay of the WPO50 fuel blends is longer, resulting in the highest BTE in all other SF mixtures. Due to the shorter combustion time and improved combustion process, the higher  $O_2$  content in the SF mixtures increases the BTE with increasing POB composition.<sup>38</sup> Sharon et al.<sup>42</sup> reported a similar trend for the BTE using n-butanol as a fuel additive. They believed that the possible reason for the BTE improvement is due to the effective combustion process, because n-butanol has a higher

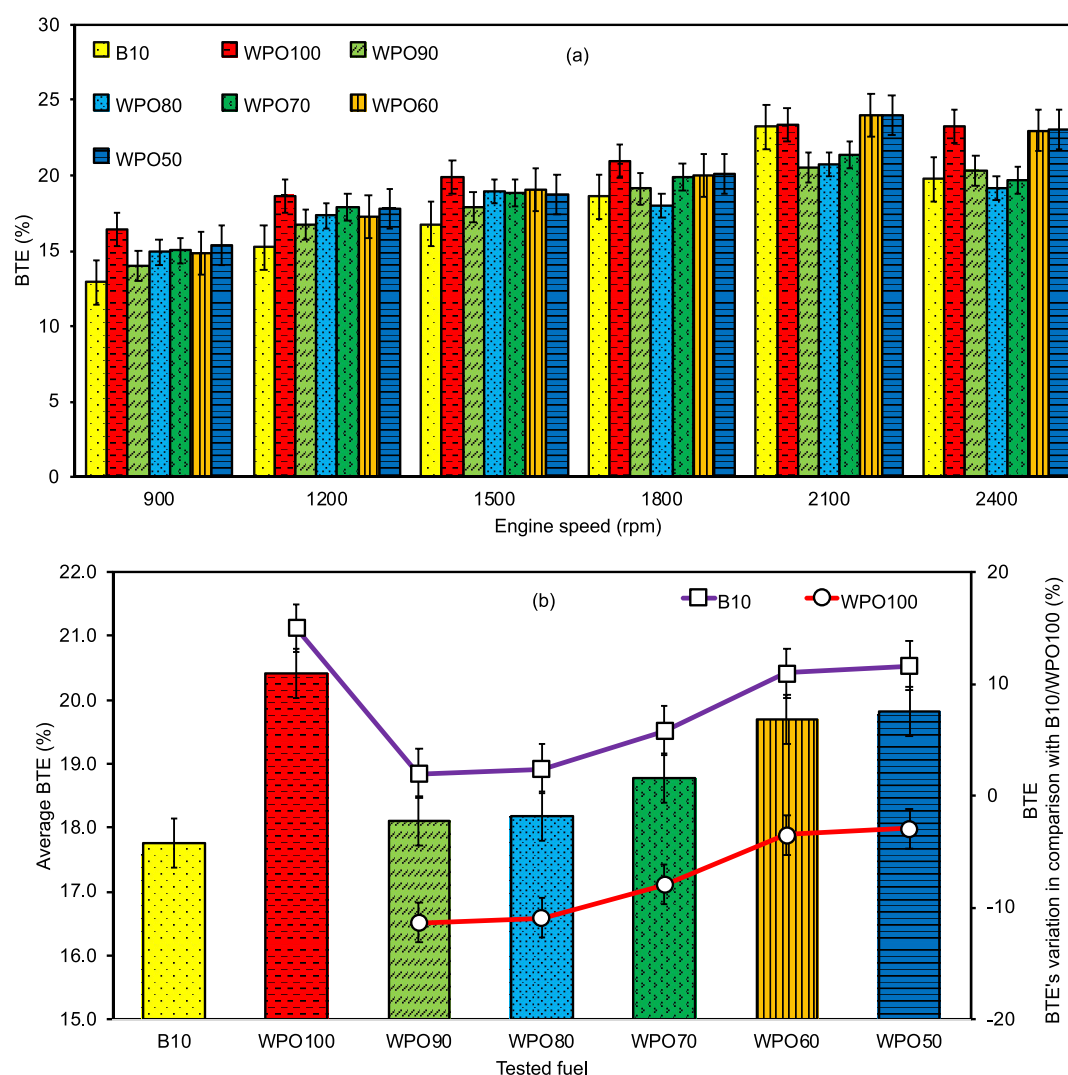


**Figure 6.** (a) Variation of BTE for all tested fuels according to engine speed at full-load condition; (b) average BTE and BTE's variation in comparison with B10 and WPO100 for the tested fuels.

O<sub>2</sub> content and thus improves the fuel–air ratio in the fuel-rich zone during the diffusion combustion process.

**2.3. Exhaust Engine Emissions.** **2.3.1. Hydrocarbon Emission.** Figure 7a shows the effect of engine speed on the HC emissions for the tested fuels. The HC emissions of all fuels were found to decrease with increasing engine speed. The maximum HC emissions of all tested fuels were recorded at a speed of 900 rpm. All fuels showed a lower amount of HC emissions when the engine speed was at the maximum compared to the low engine speed. Monirul et al.<sup>43</sup> also observed the same trend. Figure 7b shows the average value of HC emissions and the changes in HC emissions compared to B10 and WPO100. The average value of HC emissions from WPO50, WPO60, WPO100, WPO70, WPO80, B10, and WPO90 are 27.00, 28.28, 29.28, 29.56, 42.44, 43.00, and 45.33% vol, respectively. As shown in Figure 7b, the HC emission of WPO90 increased by 5.43% compared to B10 diesel. This is due to the higher viscosity in WPO90 fuel than in B10 diesel, which leads to the formation of large droplets and reduction in vapor pressure, resulting in the incomplete combustion and increased HC emissions.<sup>8</sup> Meanwhile, the HC emissions of WPO50, WPO60, WPO100, WPO70, and WPO90 decreased by 37.21, 34.24, 31.91, 31.27, and 1.29%,

respectively, compared to B10. WPO100 fuel has a lower HC emission than B10 diesel due to its low viscosity value, which leads to better atomization and combustion effect.

In addition, as shown in Figure 5c, WPO100 contains 86.02% less aromatics than B10, which extends the combustion time and shortens the ignition delay time, thereby reducing its HC emissions. Figure 7b shows that WPO70, WPO80, and WPO90 fuels show increased HC emission by 0.95, 44.97, and 54.84%, respectively, compared to WPO100. This is due to their high viscosity and density, which lead to large droplet formation, improper mixing of fuel with air, and reduction in vapor pressure, resulting in incomplete combustion and increase in HC emissions.<sup>8,44</sup> The SFs (WPO70, WPO80, and WPO90) also consist of long-chain fatty acids with higher boiling point and melting point, owing to which they are unlikely to evaporate and burn completely, thus showing increased HC emissions.<sup>25</sup> In addition, the higher HC emissions of the SFs (WPO70, WPO80, and WPO90) can be associated with their low volatility.<sup>44</sup> Nabi et al.<sup>44</sup> also found that adding up to 20% biodiesel (licella biodiesel) to diesel increased the HC emissions by approximately 13.24%. In the meantime, Kaewbuddee<sup>7</sup> observed a different trend, in which the addition of 10% POB to the WPO fuel reduced the HC



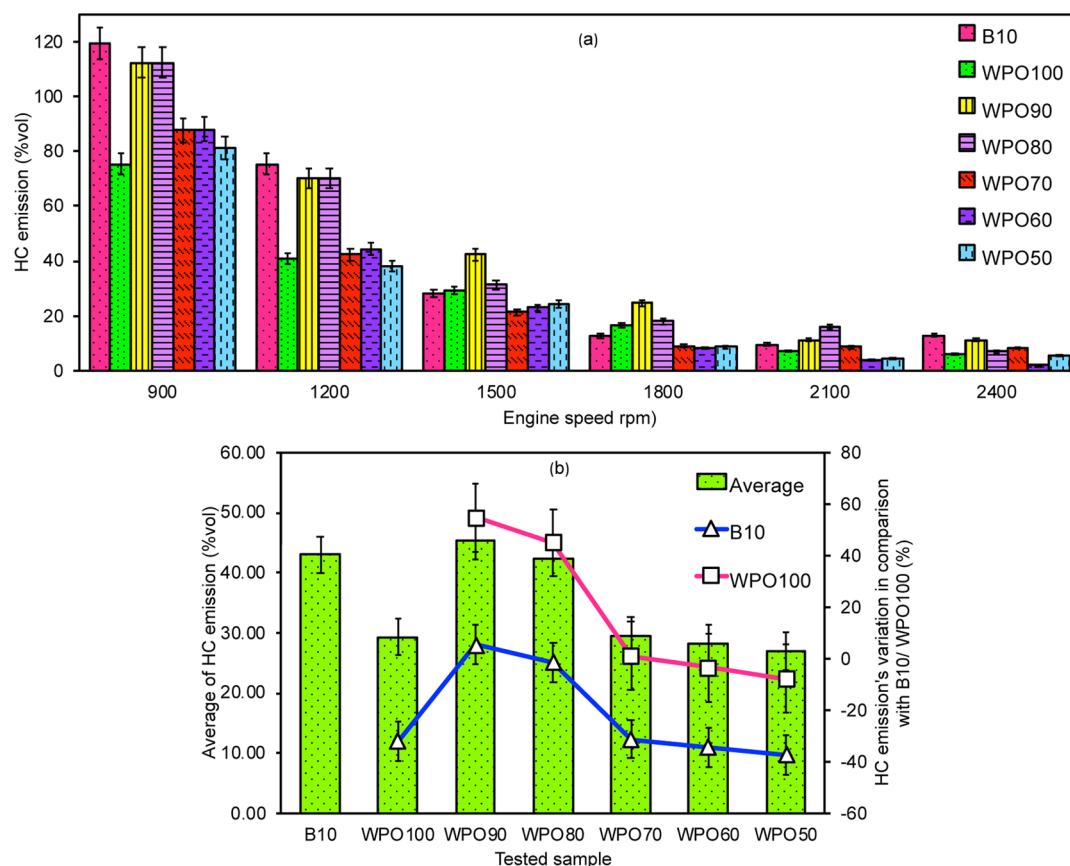


**Figure 7.** (a) Variation of HC emissions for all tested fuels according to engine speed at full-load condition. (b) HC emissions' average and variation in comparison with B10 and WPO100 for the tested fuels.

emissions by 2.12% compared to pure WPO. Meanwhile, the HC emissions from WPO50 and WPO60 fuels are 7.78 and 3.42% lower than that of WPO100. Figure 7b also shows that the HC emissions were decreased with increasing POB content in the secondary blend. These results could be attributed to the good conversion of HC, which is caused by the higher O<sub>2</sub> content in fuels, leading to the higher viscosity. This phenomenon is mainly because the biodiesel tends to provide more O<sub>2</sub> in the secondary blends, which leads to an increase in the gas temperature and reduction in possible incomplete combustion, and thereby reduction in the HC emissions.<sup>45–47</sup> These results are in good agreement with the study by Monirul et al.<sup>26</sup>

**2.3.2. Carbon Monoxide Emission.** Figure 8a shows the effect of engine speed on the CO emissions for all of the tested fuels. The maximum CO emissions of all tested fuels were recorded at a speed of 900 rpm. The CO emissions are caused by the partial combustion and partial oxidation of carbon atoms in the fuel. The amount of CO emissions varies depending on the air–fuel ratio in the engine cylinders.<sup>48</sup> The CO emissions decrease with increasing engine speed. As shown in Figure 8a, due to the high air–fuel ratio and high temperature at higher engine speeds, the rate at which CO is converted to CO<sub>2</sub> increases, thereby reducing the CO emissions. All analyzed fuel samples (WPO100, WPO50, WPO60, WPO70, WPO80, and WPO90) showed reduction in CO emission compared to B10 (commercial diesel) by 30.80, 27.10, 24.90, 22.65, 18.71, and 14.92%, respectively. WPO100 showed lesser CO emission than the B10 diesel because its lower fuel viscosity results in a better air–fuel mixing,

especially at high speeds, and the CO emissions decrease during the sufficient fuel–air mixing, which leads to complete combustion.<sup>38</sup> In addition, B10 contains a large amount of oxygenated compounds derived from 10% POB, which leads to an increase in CO emissions.<sup>8</sup> These results are in good agreement with Ruhul et al.,<sup>29</sup> who observed the same adverse effect when JB was blended with diesel.

Compared to WPO100, all SF blends (WPO50, WPO60, WPO70, WPO80, and WPO90) showed significantly increased CO emissions by 5.34, 8.52, 11.78, 17.47, and 22.95%, respectively. In Table 8, due to the combined effects of palmitic acid (C16:0) and oleic acid (C18:1), the CO emissions of B30a can be seen to be higher than those of B40 and B30a. Long-chain FAME leads to a decrease in O<sub>2</sub> content, a higher boiling point, and an increase in melting point. This leads to poor evaporation, poor combustion, and increased CO emissions.<sup>49</sup> In addition, the higher viscosity of SFs tends to result in poor fuel atomization, leading to incomplete combustion and more CO emissions. The higher viscosity could also compensate for the beneficial reduction in CO emissions due to the higher O<sub>2</sub> content.<sup>7,50</sup> Figure 8 also shows that increasing the POB composition in the SF blends reduces the CO emissions. It is the higher O<sub>2</sub> content in the SF mixtures, which causes higher viscosity, that leads to lean combustion in the cylinder and effectively improves the combustion efficiency.<sup>51,52</sup> The same trend is also observed by Kaewbuddee et al.<sup>7</sup> that the addition of 10% POB to the WPO increased the CO emissions by 8.47% compared to the blank WPO. Most researchers also found that CO emissions decreased with an increasing proportion of biodiesel.<sup>17,53–55</sup>

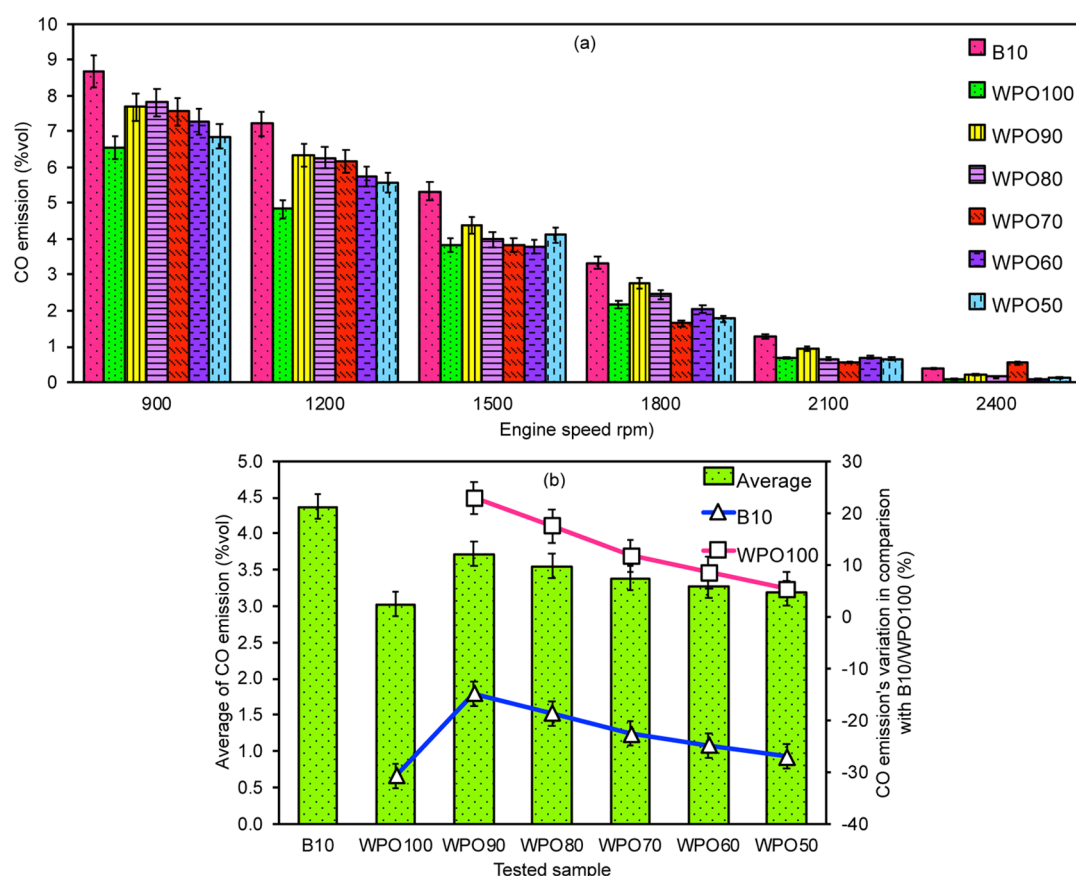


**Figure 8.** (a) Variation of CO emissions for all tested fuels according to engine speed at the full-load condition. (b) CO emissions' average and variation in comparison with B10 and WPO100 for the tested fuels.

**Table 3. Brief Comparison of the Performance and Emission Characteristics Resulted from the Present Study with Other Research Works**

type of fuel blend	ref fuel	performance				emission			ref
		BP (%)	BT (%)	BSFC (%)	BTE (%)	HC (%)	CO (%)	CO <sub>2</sub> (%)	
WPO90	WPO100	↑ 3.0	↑ 2.1	↑ 8.1	↓ 11.3	↑ 54.8	↑ 23.0	↓ 4.1	this study
WPO50		↑ 0.4	↑ 0.3	↑ 7.7	↓ 5.4	↓ 7.8	↑ 5.3	↑ 8.8	
90% WPO + 10% POB	WPO			↑ 1.3	↓ 2.2	↓ 2.1	↑ 8.5		Kaewbuddee et al. <sup>7</sup>
90% WPO + 10% castor oil biodiesel				↑ 1.7	↓ 2.1	↓ 3.5	↑ 15.3		
90% WPO + 10% Jatropha oil biodiesel	WPO			↑ 5.5	↑ 4.8		↓ 22.8		Senthilkumar and Sankaranarayanan <sup>17</sup>
90% diesel + 10%POB	diesel	↓ 0.5		↑ 1.0	↑ 1.4				Ali et al. <sup>22</sup>
90% diesel + 10%POB	diesel			↑ 33.3	↓ 25.5	↓ 14.5			Kumar et al. <sup>63</sup>

**Table 4. Brief Comparison of COF and WSD Resulted from the Present Study with Other Research Works**

fuel sample	composition	reference fuel	COF (%)	WSD (%)	ref
WPO90	90% WPO + 10% WPO	WPO100	↑ 7.0	↓ 4.8	current study
WPO50	50% WPO + 50% WPO		↑ 2.5	↑ 14.5	
WPO10	90% WPO + 10% POB		NA	↓ 1.1	Kaewbuddee et al. <sup>7</sup>
WPOC10	90% WPO + 10% castor oil biodiesel		NA	↓ 1.9	
B50	50% POB + 50% diesel fuel		↓ 3.74	↓ 12.18	Fazal et al. <sup>59</sup>
POME50	50% POB + 50% diesel fuel		↓ 13.90	NA	Jamshaid et al. <sup>64</sup>
CPME50	25% castor oil biodiesel + 25% POB and 50% diesel		↓ 10.4	NA	
B30	30% palm–sesame oil biodiesel + 70% diesel		↓ 31.10	↓ 43.27	Mujtaba et al. <sup>65</sup>

**2.3.3. Carbon Dioxide Emission.** CO<sub>2</sub> emission is the result of complete combustion in which the carbon atoms contained in the fuel are completely oxidized. It is generally not regulated by emission legislations and is not considered a harmful gas.

However, since it is a greenhouse gas, there is a strong need to reduce CO<sub>2</sub> emissions.<sup>8,10</sup> Figure 9a,b shows the CO<sub>2</sub> emissions of all of the tested fuels. Figure 9a shows the increasing trend of CO<sub>2</sub> emissions for all mixtures with

Table 5. Composition of SF Blends

sample Code	fuel composition (by volume)
WPO90	90% WPO and 10% POB
WPO80	80% WPO and 20% POB
WPO70	70% WPO and 30% POB
WPO60	60% WPO and 40% POB
WPO50	50% WPO and 50% POB

increasing speed. The average CO<sub>2</sub> emissions from WPO50, WPO60, WPO70, B10, WPO100, WPO80, and WPO90 were 9.97, 9.46, 9.45, 9.43, 9.16, 9.09, and 8.79% vol, respectively. Compared to B10, the CO<sub>2</sub> emissions of WPO50, WPO60, and WPO70 increased on average by 5.77, 0.29, and 0.22%, respectively. The same trend was observed by Sivakrishna, Madhu, and Sivakumar.<sup>56</sup> They pointed out that using POB (20–40%) in diesel will increase the CO<sub>2</sub> emissions compared to blank diesel.

Meanwhile, the CO<sub>2</sub> emissions of WPO90, WPO80, and WPO100 decreased by 6.78, 3.60, and 2.82%, respectively, compared to B10 diesel. WPO100 fuel has fewer CO<sub>2</sub> emissions than B10 due to its lower BSFC than B10, which is caused by a lower BTE, dominating the presence of higher carbon number compounds in WPO100 than in B10 diesel.<sup>11,44</sup> Kumar et al.<sup>13</sup> also found that the WPO's CO<sub>2</sub> emission is 11.39% lower than that of blank diesel and WPO–diesel blends. This result indicates a positive environmental impact when using WPO as a fuel. However, most studies reported that WPO caused higher CO<sub>2</sub> emissions than

diesel.<sup>10,11,14</sup> Compared to WPO100, the CO<sub>2</sub> emissions from WPO90 and WPO80 decreased by 4.07 and 0.81%, respectively, while the CO<sub>2</sub> emissions from WPO70, WPO60, and WPO50 increased by 3.12, 3.20, and 8.83%, respectively. As shown in Figure 9b, increasing the POB composition in the SF blends increases the CO<sub>2</sub> emissions. The main reason for the higher CO<sub>2</sub> emissions is the higher O<sub>2</sub> content in the fuel mixture, which leads to complete combustion of fuel and high temperature in the cylinder.

**2.4. HFRR Tribological Study.** Figure 10a shows the COF trend of all fuel samples tested by HFRR over time. In the early stages of the experiment, the COFs of all samples were high because there was no lubricating film between the contact surfaces. It is called the running-in period. A lubricating film forms between the mating surfaces, and the surface roughness between the friction surfaces becomes smoother over time. This phase of the experiment is called the steady-state condition.<sup>57</sup> The B10 fuel sample showed a low running-in period. The results show that the wear and friction decrease with increasing POB concentration in the SFs. Figure 10a,10b shows the average values of COF and WSD of all tested samples and their changes compared to B10 and WPO100. The average COF values of all analyzed samples (B10, WPO100, WPO50, WPO60, WPO70, WPO80, WPO90, and POB100) were 0.0657, 0.0693, 0.0710, 0.0728, 0.0733, 0.0740, 0.0742, and 0.0747, respectively. The WSD values of all analyzed samples (WPO90, WPO80, WPO100, POB100, B10, WPO70, WPO60, and WPO50) were 1.121, 1.139, 1.178, 1.246, 1.250, 1.325, 1.334, and 1.348 mm, respectively. POB

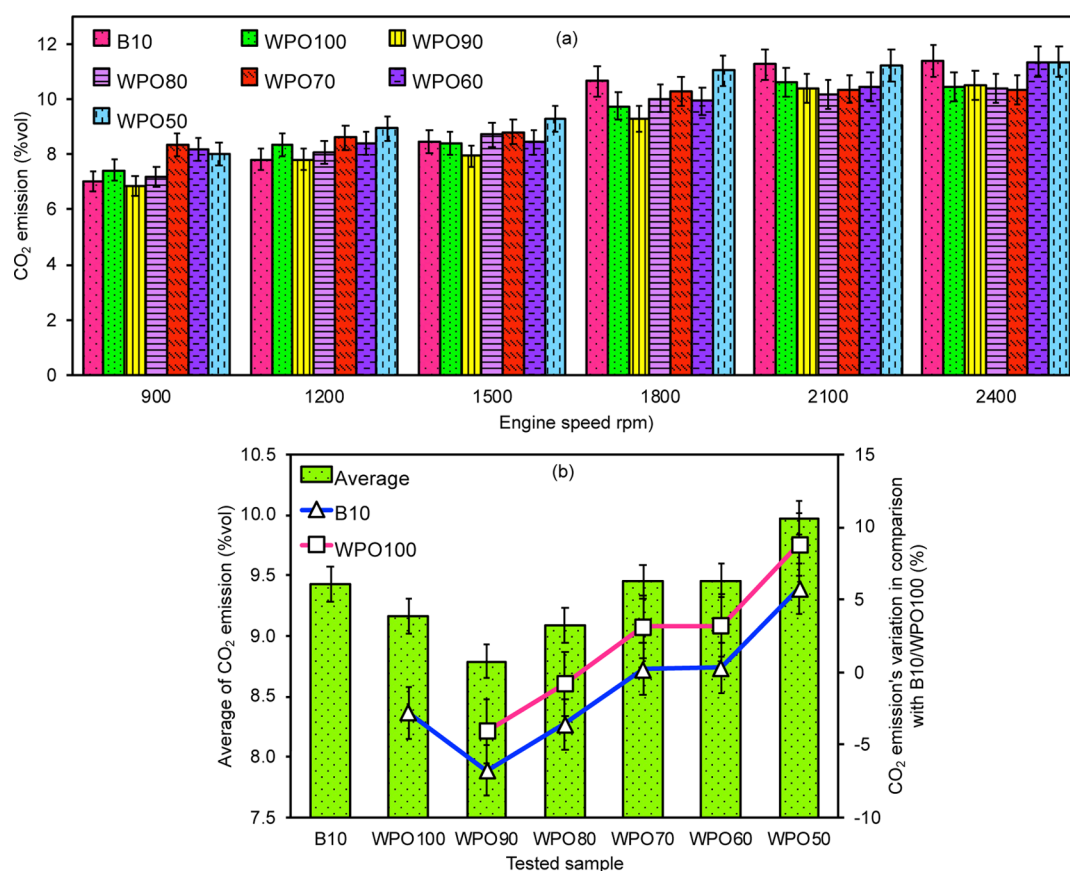


**Figure 9.** (a) Variation of CO<sub>2</sub> emissions for all tested fuels according to engine speed at the full-load condition. (b) CO<sub>2</sub> emissions' average and variation in comparison with B10 and WPO100 for the tested fuels.

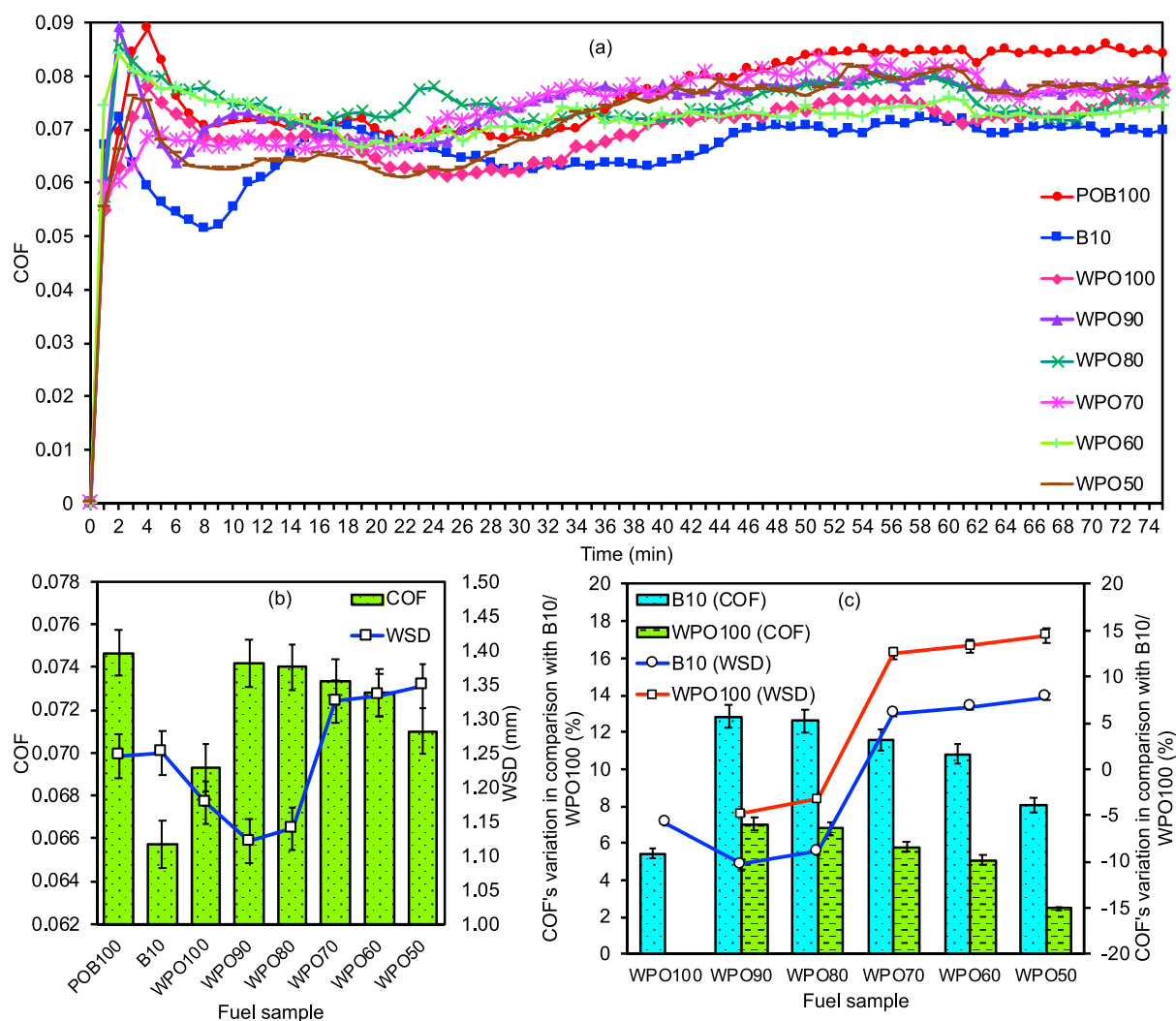


**Figure 10.** (a) COF during the run-in period and steady-state period, (b) average COF and WSD, and (c) variation of COF and WSD in comparison with B10 and WPO100 for all tested fuel samples by HFRR.

**Table 6. Physicochemical Properties of B10, WPO100, POB100, and SF Blends**

properties of test fuel	test method	B10	POB100	WPO100	WPO90	WPO80	WPO70	WPO60	WPO50
density at 15 °C (kg/m <sup>3</sup> )	ASTM D 4052	0.8026	0.936	0.832	0.8102	0.8175	0.8252	0.8323	0.8391
kinematic viscosity at 40 °C (mm <sup>2</sup> /s)	ASTM D 445	2.9181	5.5932	2.905	3.0073	3.109	3.228	3.3882	3.556
kinematic viscosity at 100 °C (mm <sup>2</sup> /s)	ASTM D 445	1.2449	1.7414	1.1999	1.2799	1.3134	1.3435	1.3958	1.4148
dynamic viscosity at 40 °C (mPa·s)	ASTM D 445	2.2901	3.9642	2.3649	2.3824	2.4854	2.6058	2.7583	2.9218
dynamic viscosity at 100 °C (mPa·s)	ASTM D 445	0.92366	1.4158	0.92521	0.95859	0.99282	1.0293	1.0754	1.1034
viscosity index	ASTM D 2270	282.6	183.9	167.5	281.8	267.8	239.6	231.2	178.7
calorific value (MJ/kg)	ASTM D 240	45.828	39.98	45.614	44.511	44.452	44.295	42.489	42.469
flash point (°C)	ASTM D 93	40	174	80	44	50	53	59	61
oxidation stability at 110 °C (induction time/h)	ASTM D 7462	37.56	3.96		22.38	13.93	7.64	5.15	4.35

showed the highest COF among the tested fuels because of the oxidation process, which converts the esters into various fatty acids, including formic acid, acetic acid, propionic acid, caproic acid, etc.<sup>58</sup> The polyunsaturated content in POB, such as oleic

acid (Table 8), could be the most powerful factor that influences the auto-oxidation. The oxidation process can lead to fuel degradation, which causes reduced lubricity, enhanced corrosion, and material deterioration.<sup>59</sup>

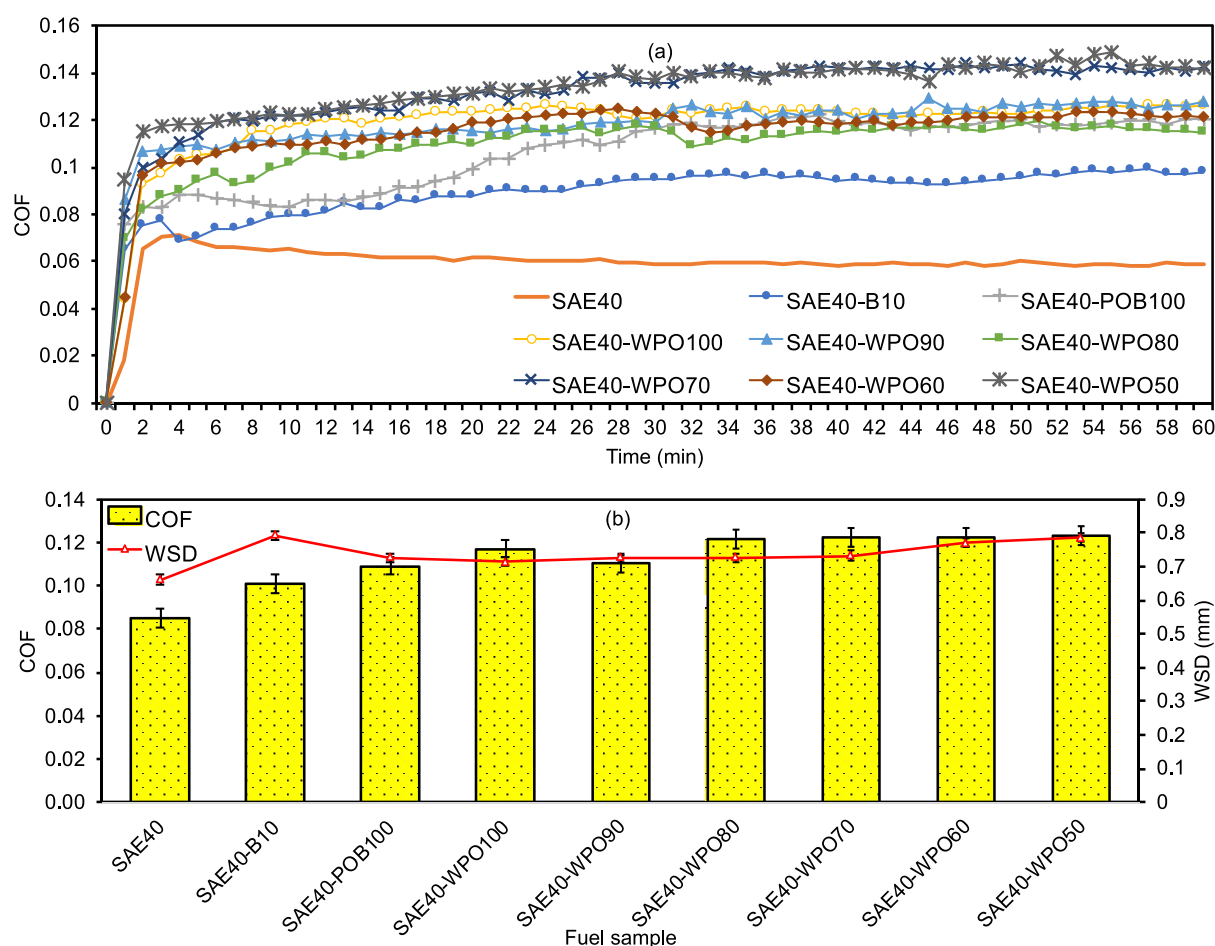


**Figure 11.** (a) COF during the run-in period and steady-state period; (b) average COF and WSD for the mineral lubricant and lubricant-contaminated samples.

Compared to B10 diesel, the COF increments in WPO100, PO50, WPO60, WPO70, WPO80, and WPO90 are 5.44, 8.02, 10.80, 11.53, 12.59, and 12.84%, respectively. The WSD of WPO90, WPO80, and WPO100 decreased by 10.34, 8.86, and 5.80%, respectively, while the WSD of WPO70, WPO60, and WPO50 increased by 6.01, 6.72, and 7.82%, respectively, compared to B10. Compared to WPO100, the COF of WPO50, WPO60, WPO70, WPO80, and WPO90 increased by 2.45, 5.08, 5.78, 6.78, and 7.02%, respectively. WPO100 showed a lower COF than the secondary blend fuels because of its lower viscosity, which minimizes engine friction.<sup>20</sup> Figure 10b shows that the increasing POB composition in SF blends lowers the COF value due to the higher concentration of FAME, where the fatty acids create a protective layer between the contact surfaces that counteracts the adverse effects of unsaturated fatty acids.<sup>23,60</sup>

However, Figure 10b shows that the WSD value increased with increasing POB composition in SF blends, with the WSDs of WPO90 and WPO80 being 4.82 and 3.25%, respectively, lower than that of WPO100, and those of WPO70, WPO80, and WPO90 being 12.54, 13.29, and 14.46% higher than that of WPO100, respectively. This phenomenon is known as oxidative corrosion, which is caused by the various acids that are produced when the esters in POB are oxidized. WPO90 shows the lowest WSD among the secondary blends. It can be concluded that 10% biodiesel was sufficient to maintain the lubrication of the mixed fuel, and there was no significant

improvement in the lubrication of the mixture by exceeding this percentage of POB in WPO. The same observation was made by Kaewbuddee et al.,<sup>7</sup> that the presence of 10% POB in WPO is the optimal ratio, since it gives the smallest WSD (0.32 mm) among other tested fuels (5% POB in WPO, 0.32 mm; 15% POB in WPO, 0.33 mm).

**2.5. Four-Ball Tribological Study.** The effect of different fuel samples on the lubricity of mineral lubricant is shown in Figure 11. According to the previous literature, the lubricant is contaminated with fuel by up to 5% due to the thinning of the crankcase.<sup>61</sup> The lubricant was contaminated with combustible fuel, which changed the tribological properties of the lubricant and resulted in poor lubricating properties due to the degradation of the lubricant. Figure 11a shows the COF trends for all tested samples. The running-in-period of the pure mineral lubricant was much shorter due to its better lubricating properties. The steady-state conditions were reached quickly due to the formation of the lubricating film between the metallic contacts in the initial phase of the experimental run.<sup>43</sup> The mineral lubricant showed a much lower COF (0.0850) compared to other contaminated lubricant samples with different fuels (0.1013–0.1231). The same trend was observed by Masjuki and Maleque.<sup>62</sup> They reported that more than 5% POB in the lubricant caused oxidation and corrosion. The addition of combustible fuel to the lubricant changed its lubricating properties and resulted in poor tribological performance.

Table 7. Physicochemical Properties of the Tested Lubricant Fuel Samples

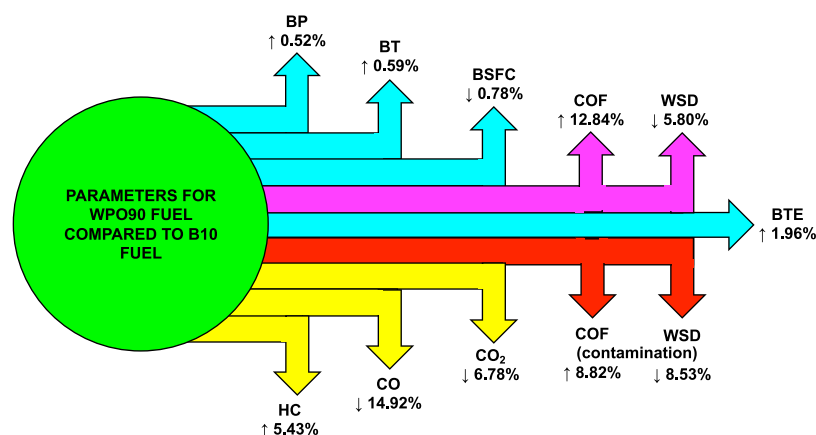
properties of test fuel	100% lubricant (SAE40)	SAE40 + 5% POB100	SAE40 + 5% B10	SAE40 + 5% WPO100	SAE40 + 5% WPO90	SAE40 + 5% WPO80	SAE40 + 5% WPO70	SAE40 + 5% WPO60	SAE40 + 5% WPO50
density at 15 °C (kg/m <sup>3</sup> )	894.1	892.4	895.4	889.8	890.9	890.7	889.4	890.7	891.3
kinematic viscosity at 40 °C (mm <sup>2</sup> /s)	129.63	98.15	129.44	95.23	99.58	98.12	95.17	96.95	97.94
kinematic viscosity at 100 °C (mm <sup>2</sup> /s)	13.33	11.56	11.62	11.24	11.45	12.08	11.21	11.34	11.46
dynamic viscosity at 40 °C (mPa·s)	113.86	86.04	113.68	83.23	87.13	85.84	83.17	84.82	85.74
dynamic viscosity at 100 °C (mPa·s)	11.21	9.70	9.73	9.39	9.58	10.11	9.37	9.49	9.60
viscosity index	96.9	105.5	70.0	100.0	101.7	114.5	100.0	103.5	104.1

Figure 11a also shows that the mineral lubricant contaminated with blank WPO and SF mixtures exhibited greater lubricant degradation than B10. The average COFs of SAE40-WPO100, SAE40-WPO90, SAE40-WPO80, SAE40-WPO70, SAE40-WPO60, and SAE40-WPO50 are higher than that of SAE40-B10 by 15.74, 8.82, 20.25, 20.84, 20.97, and 21.51%, respectively. All contaminated lubricant samples showed high COFs due to the decrease in viscosity, which had a large impact on the fuel lubricity, compared to the mineral lubricant. Among secondary contaminated samples, SAE40-WPO90 showed the best COF with a reduction of 5.98% compared to SAE40-WPO100 due to the presence of ester molecules. However, the COFs for other secondary contaminated samples (SAE40-WPO80, SAE40-WPO70, SAE40-WPO60, and SAE40-WPO50) increased by 3.89, 4.41, 4.52, and 4.98%, respectively, compared to SAE40-WPO100. Thus, increasing the POB content in the secondary contaminated sample increased the COF. The same trend is also seen for the WSD. All secondary contaminated lubricant samples showed an increment in WSD of 1.66, 1.75, 2.65, 7.84, and 10.17% for SAE40-WPO90, SAE40-WPO80, SAE40-WPO70, SAE40-WPO60, and SAE40-WPO50, respectively, compared to SAE40-WPO100.

**2.6. Comparative Study.** To better confirm and explain the experimental results, similar studies were reviewed. Table 3 shows the effects of various WPO–biodiesel and diesel–biodiesel mixtures on the performance and emission characteristics of diesel engines, derived from the results of this study and other publications. In terms of the performance of diesel engines like BP, BSFC, and BTE, this study shows trends that are almost similar to most previous studies. However, Senthilkumar and Sankaranarayanan<sup>17</sup> observed that adding 10% JB to WPO improves the BTE by 4.8% compared to pure WPO due to its superior properties (low viscosity and higher calorific value) than POB fuel. Ali et al.<sup>22</sup> also reported the same results in their study in which they examined the performance of the POB–diesel mixture in diesel engines.

Similarly, the CO, CO<sub>2</sub>, and HC emission characteristics of the current study show the same trend as most of the previous studies. Kaewbuddee et al.<sup>7</sup> conducted a study to investigate the impact of WPO–POB and WPO–castor oil biodiesel blends on diesel engine performance and emission characteristics. However, their results do not agree well with the current study because they reported that adding 10% biodiesel to WPO helped to reduce the HC emission. Kumar et al.<sup>63</sup> also reported the same results in their study that examined the operation of the diesel–POB mixture in diesel engines. In this study, it is possible to reduce the HC emission by increasing the POB content in the secondary blend from 10 to 50%. It is because the higher O<sub>2</sub> content of the SF tends to decrease the HC emission and counteracts the disadvantageous increment in HC emissions due to the higher viscosity. In addition, Senthilkumar and Sankaranarayanan<sup>17</sup> reported that JB succeeded in reducing the CO emissions by 22.8% compared to blank WPO. The reason for this may be that the excess O<sub>2</sub> present in JB is helpful for better combustion. Therefore, JB could be a great candidate for making a ternary blend (WPO–POB–JB blend) to minimize the CO emission.

Table 4 briefly lists the COF and WSD values that were derived from this research and other research findings. For WSD, similar trends were obtained for the addition of 10% POB to POB. No study reports the effect of adding biodiesel in WPO on the COF. Most studies have agreed that adding up to



**Figure 12.** Average percent change in the parameters measured for WPO90 fuel compared with B10 diesel fuel.

50% biodiesel to diesel fuel improves the lubricity and tribological properties, resulting in a lower COF and WSD compared to diesel fuel.

**2.7. Limitations of the Secondary Blend Fuel.** Figure 12 shows the summary of the average parameter changes of the WPO90 fuel compared with B10 diesel. WPO90 shows better overall diesel engine performance and emission characteristics than B10 with BP, BT, and BTE values increased by 0.52, 0.59, and 1.96%, respectively, and BSFC decreased by 0.78%. To further improve the diesel engine performance, Mujtaba et al.<sup>30</sup> suggested using oxygenated alcohols such as dimethyl carbonate (DMC) and diethyl ether (DEE) in the fuel blends. Compared to B10 diesel, the CO and CO<sub>2</sub> emissions of WPO90 decreased by 14.92 and 6.78%, respectively, while the HC emission of WPO90 slightly increased by 5.43%. WPO90 shows an increment of COF by 12.84 and lubricant contamination by 8.82% compared to B10 diesel. The addition of nanoparticles to fuel mixtures can improve the lubricity and tribological properties, which leads to a lower COF compared to fuel samples without nanoparticles.<sup>23,65</sup> This is because the nanoparticles act as a sacrificial layer between the friction surfaces. Razzaq et al.<sup>23</sup> reported that graphene oxide nanoplatelets with diesel–biodiesel–alcohol fuel blends showed a lower COF due to the presence of nanoparticles between metallic contacts. The same observation was made by Mujtaba et al.,<sup>65</sup> who used titanium oxide nanoparticles in the mixtures of palm–sesame methyl ester–diesel.

### 3. CONCLUSIONS

To investigate the impact of POB in WPO on the engine performance, emission, and lubrication characteristics, five SF mixes were created. Based on the findings, the following conclusions are drawn.

- With the exception of WPO80, which exhibited a 2.75% drop in BTE, the BTE values for SF mixes were greater than B10. Among the SF blends, WPO90 had the highest BP and BT.
- The BSFC of the SF mixes was lower than that of B10 diesel, with the exception of WPO80, which had a 3.61% higher BSFC.
- The effect of increasing the POB percentage on BP and BT was insignificant.
- WPO50 (37.21%) and WPO90 (6.78%) achieved the highest reductions in HC and CO<sub>2</sub> emissions when compared to B10, respectively.

- WPO50 among the SF blends had the highest decrease in CO emissions of 27.10% when compared to B10.
- The COF of all SF blends was greater than that of B10 diesel and WPO100. When compared to WPO100, WPO50 showed the smallest COF increase of 2.45%. WPO90, on the other hand, showed the greatest WSD decrease of 10.34% when compared to B10.
- When compared to SAE40-WPO100, SAE40-WPO90 had the lowest COF value, with a reduction of 5.98%. The COF values rose as the POB concentration in the SF-contaminated sample increased. Regarding the WSD values, the same patterns were found.

Thus, these factors strongly support the fact that WPO combined with POB appears to be a viable fuel for diesel engines that does not require any engine modifications, as it has high efficiency, lower emissions, and enhanced wear characteristics. WPO mixed with POB has also been proven to be a good diesel substitute, with WPO90 being the best SF combination with a great potential for diesel engine performance. The advantages of POB were examined, such as the high O<sub>2</sub> concentration in fuel molecules. The presence of O<sub>2</sub> in the fuel molecules helps to improve the combustion processes in terms of performance and emissions. In the future, secondary blends containing oxygenated alcohols and nanoparticles will be investigated in diesel engines to improve the diesel engine and wear characteristics.

### 4. MATERIALS AND METHODS

WPO was produced by Syngas Sdn Bhd, Kuala Lumpur, Malaysia; meanwhile, POB and B10 were purchased from KL-Kepong Oleomas Sdn Bhd, Selangor, Malaysia, and Petron Jalan Universiti, Kuala Lumpur, Malaysia, respectively. In the current study, a blend of WPO–POB was used to prepare the SFs, and B10 and WPO100 were used as the reference oils. In accordance with the ASTM D6079-11 dimensions, AISI 52100 Chrome hard-polished steel balls with a diameter of 6.2 mm, 15-mm SAE-AMS 6440 steel smooth diamond polish discs, and 12.7-mm-diameter AISI 52100 steel balls with a hardness of 64–66 Rc were bought from the local market.

**4.1. WPO Production.** The polypropylene and polyethylene (PP–PE) wastes were collected and processed into granules. The conversion of PP–PE granules into WPO was carried out by pyrolysis in the absence of O<sub>2</sub>, the catalytic reforming, and the condensation of the resulting gases. A portable semibatch-type reactor was utilized. The PP–PE

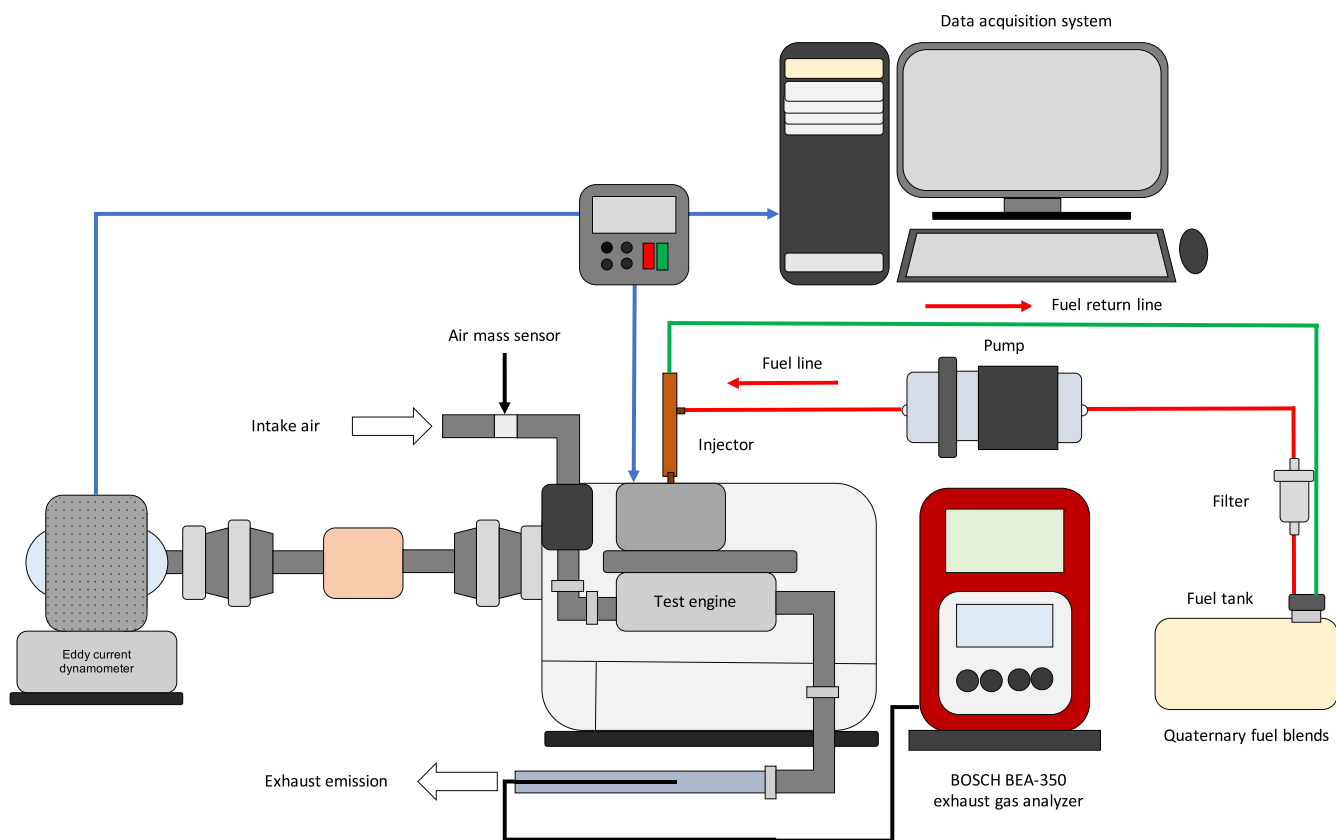


**Figure 13.** Schematic view of the diesel engine setup.

granules were exposed to steam and then processed into molten plastic. The molten plastic was heated in the pyrolysis reactor at a controlled temperature (500 °C). Then, it was flown through the catalytic chamber under the force of vaporizing pressure. The gaseous product was further cracked in the catalytic chamber and then expelled through the vent. After passing through the chamber, condensation and distillation of gaseous product occurred. The condensed oil (WPO) was then stacked in the storage tank.

#### 4.2. Gas Chromatography and Mass Spectrometry.

The WPO, POB, and B10 were analyzed by gas chromatography and mass spectrometry (GC–MS) using a Hewlett-Packard HP 7890 equipped with a 5975 quadrupole detector. The capillary column of the gas chromatograph is measured at a length of 30 m and a diameter of 0.25 mm, and is covered with 0.25  $\mu\text{m}$  of a 5% phenyl methyl polysiloxane (HP-5) film. The initial oven temperature was set to 50 °C at a 2 min interval, then increased to 290 °C at a rate of 5 °C/min, and held isothermal for 10 min. The ion source and transmission line temperature were maintained at 230 and 300 °C, respectively, and the splitless injection temperature was maintained at 290 °C. Data were collected in a full-scan mode between  $m/z$  33 and 533, and a solvent interval of 3 min was used. Chromatographic peaks were identified by the NIST08-based mass spectrum database or the reaction time of standard compounds. They were calculated from the peak area of the total ion chromatogram. These methods were adapted from Juwono et al.<sup>66</sup>

#### 4.3. Fuel Sample Preparation. 4.3.1. Fuel Sample Preparation for HFRR and the Engine Test Rig.

Several fuel samples were prepared to examine the lubricity of the fuel and

the effect of SF mixtures on the characteristics of the diesel engine. The prepared fuel samples were compared to commercially available Malaysian diesel (B10). WPO was mixed with POB to make various SF compositions as shown in Table 5. Those SF mixtures were stirred at 700 rpm for half an hour until they became homogeneous. The physicochemical properties of B10, WPO100, and POB (POB100), as well as the SF blends are listed in Table 6. The physicochemical properties of WPO–POB biodiesel and B10 were estimated according to the standard biodiesel methods (ASTM D6751 and EN 14214).

**4.3.2. Lubricant Sample Preparation.** Firstly, 5% of each of the fuels listed in Table 6 were mixed with commercial SAE40 lubricant using a magnetic stirrer at a speed of 900 rpm for 30 min, since the lubricant mixing with the fuel occurred at 5% due to the dilution of the crankcase.<sup>67</sup> The physicochemical properties of the SAE40 reference lubricant and all other lubricant samples with different fuels were measured using a viscometer (SVM 3000) as shown in Table 7.

**4.4. Experimental Setup. 4.4.1. Experimental Setup of the Diesel Engine.** The study on the attribute diesel engine from various fuel samples in this present study was carried out by using a diesel engine test bed (model: Yanmar (TF 120 M)) from the University of Malaya. The schematic diagram of this diesel engine test rig and its specification description are represented in Figure 13 and Table 8, respectively.

To study the features of the internal combustion engine, the fuel flow rate of B10 was measured. By using a graduated measuring cylinder, three readings and their average per 10 mL of fuel samples were recorded at every engine speed tested. In the meantime, the time taken was recorded by a stopwatch.



**Table 8.** Engine Specifications Used for the Experimental Work

engine specification	description
no. of cylinders	1
aspiration	radiator cooling
cylinder bore × stroke (mm)	92 × 96
displacement (L)	0.638
compression ratio	17.7
maximum engine speed (rpm)	2400
maximum power (kW)	7.7
injection timing (deg)	17° BTDC
injection pressure (kg/cm <sup>2</sup> )	200
power take-off position	flywheel side
cooling system	radiator cooling
connecting rod length (mm)	149.5

Then, the DAPSTEP8 software was used to analyze both the BT and the BP. Table 9 summarizes the specifications of the

**Table 9.** Gas Analyzer Specifications

equipment	method	measurement	measurement range	resolution
BOSCH	infrared	HC	0–9999 ppm	1 ppm
BEA 350	pulsating light	CO	0–10% vol	0.001% vol
		CO <sub>2</sub>	0–18% vol	0.01% vol

engine gas emissions (HC, CO, CO<sub>2</sub>, and O<sub>2</sub>), which were determined by a BOSCH gas analyzer. These methods were adapted from the study by Mujtaba et al.<sup>30</sup> However, NO<sub>x</sub> could not be measured due to the limitation of the gas analyzer.

Firstly, a diesel engine was used to operate the B10 fuel sample so that the operation could be kept in stable conditions. Next, to examine the characteristics of the engine, the diesel engine was loaded with WPO100 and SF blends. The fuel samples tested were B10, WPO100, WP090, WPO80, WPO70, WPO60, and WPO50. Under the full-load condition (100%), 7 different speeds (900, 1150, 1400, 1650, 1900, 2150, and 2400

rpm) were used to operate the experimental test rig diesel engine. For all engine parameters (BSFC, BP, BT, BTE, CO, HC, and CO<sub>2</sub>), the relative uncertainty percentages  $u_p$  were calculated from different uncertainties of the equipment. The formula in eq 1 below was used to predict the overall uncertainty of the experiments,  $u_{\text{overall}}$ :

$$u_{\text{overall}} = \sqrt{u_{\text{BSFC}}^2 + u_{\text{BTE}}^2 + u_{\text{BP}}^2 + u_{\text{CO}}^2 + u_{\text{CO}_2}^2 + u_{\text{HC}}^2}$$

$$= \sqrt{(1.3)^2 + (0.3)^2 + (0.7)^2 + (1)^2 + (1)^2 + (1)^2}$$

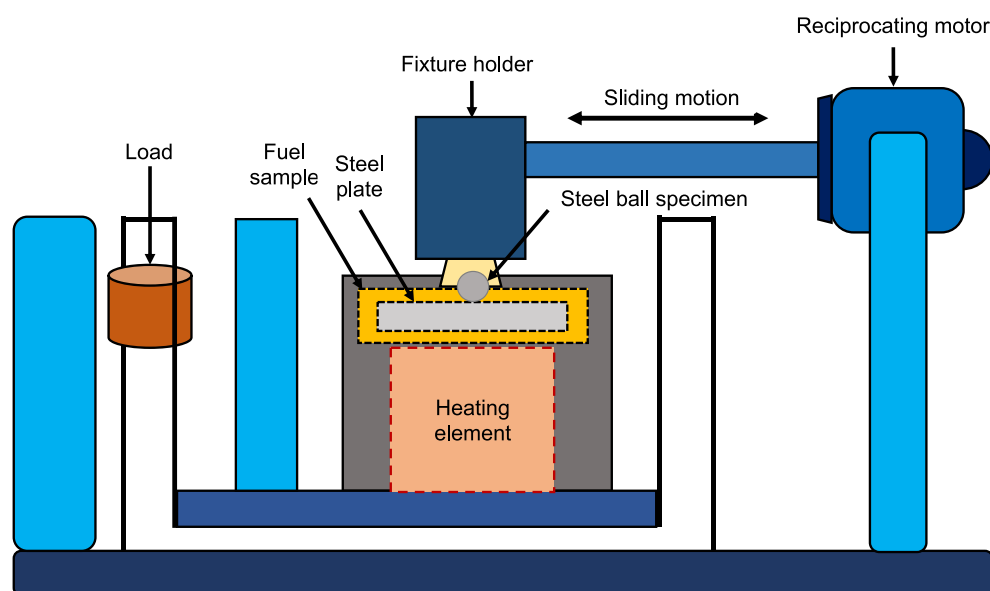
$$= \pm 2.23\% \quad (1)$$

**4.4.2. HFRR Test Rig.** A DUCOM's HFRR equipment (model: TR-281-M8) was used to evaluate the eight fuel samples as shown in Figure 14. Several specimens were cut at 15 mm × 15 mm dimensions to serve as the test sample plates, and they were polished with 600, 800, 1000, 1500, and 2000 silicon carbide papers using a polishing machine. Next, as a layer of additional polish, a 1 μm × 3 μm diamond suspension was applied onto the specimens. Then, a profilometer (Veeco Dektak 150) was used to measure the surface roughness, and it was kept in the range of 0.03–0.04 (R<sub>a</sub>). To investigate the tribological behavior of the fuel samples, a ball on a test sample plate was used, in which the steel ball is let to slide on a steel specimen, submerged in a 5.0 ± 0.2 mL fuel sample in a reciprocating motion. The operating conditions during the tribology test summarized in Table 10 are based on the

**Table 10.** HFRR Tribological Test Operating Conditions

test parameters	standard value
sample temperature	60 °C
sample test duration	75 min
applied load	5 N
frequency	10 Hz
stroke length	2 mm
sample volume	10 mL

standard test method ASTM D6079-11. The conditions are kept as follows: a stroke length of 2.0 ± 0.02 mm, a frequency

**Figure 14.** Schematic view of the reciprocating friction and wear monitor (HFRR) rig.

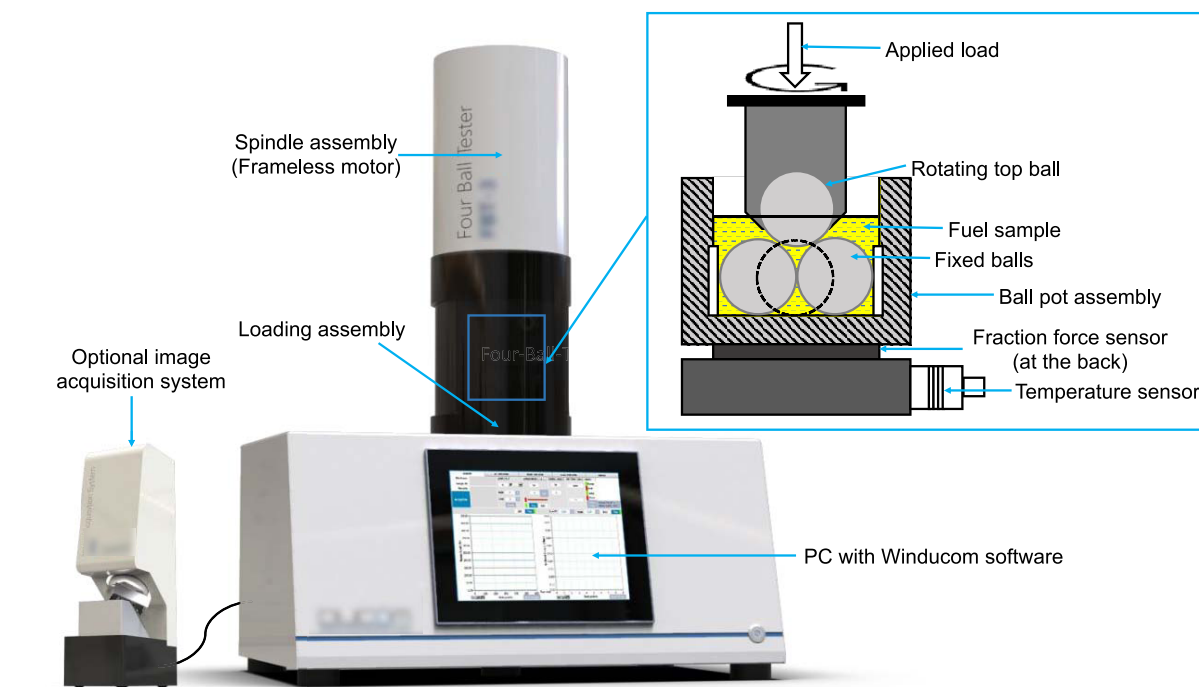


Figure 15. Schematic view of the four-ball test rig.

of  $10.0 \pm 1$  Hz for 75 min, an applied load of  $5 \pm 0.01$  N, and a constant fuel temperature of  $60 \pm 2$  °C. These methods were adapted from the study from Mujtaba et al.<sup>65</sup>

After the tribological experiments had been carried out, optical microscopy (OM) was used to calculate the WSD of both the worn steel ball and the steel plate. The WSD of the worn surfaces and the COF were measured using eqs 2 and 3 shown below, respectively:

$$\text{WSD} = \frac{M + N}{2} \quad (2)$$

in which  $M$  is the major axis (in  $\mu\text{m}$ ) measured through OM and  $N$  is the minor axis (in  $\mu\text{m}$ ) measured through OM.

$$\text{COF} = \frac{\text{actual frictional force (N)}}{\text{applied load (N)}} \quad (3)$$

**4.4.3. Four-Ball Tribo Tester Rig.** The relationship between various fuels and their effects on the tribological properties of the lubricant was examined by using a four-ball tribo tester (FBT-3, Ducom Instruments, Bengaluru, India) as illustrated in Figure 15. Firstly, the cup holder that contained three stationary steel balls was attached to a temperature sensor and then filled with 10 mL of the lubricant sample. For every experiment tested, four new separated steel balls were used. The working conditions in this study as summarized in Table 11 were used throughout all of the tests carried out in this study, which are in accordance with the standard test method

Table 11. Four-Ball Tribological Test Operating Conditions

test parameters	standard value
test duration	60 min
applied load	40 kg
oil temperature	75 °C
rotational speed of the spindle	1200 rpm

ASTM D4172. Next, the WSD of the steel ball was measured right after the tribological experiments using an OM. The WSD of the worn surfaces and the COF were computed using eqs 2 and 3.<sup>65</sup>

## AUTHOR INFORMATION

### Corresponding Authors

**Muhamad Sharul Nizam Awang** – Department of Mechanical Engineering, Faculty of Engineering, Universiti Malaya, 50603 Kuala Lumpur, Malaysia; [orcid.org/0000-0002-7733-6560](https://orcid.org/0000-0002-7733-6560); Phone: +60379674462; Email: [17202353@siswa.um.edu.my](mailto:17202353@siswa.um.edu.my)

**Nurin Wahidah Mohd Zulkifli** – Department of Mechanical Engineering, Faculty of Engineering, Universiti Malaya, 50603 Kuala Lumpur, Malaysia; Centre for Energy Sciences (CFES), Department of Mechanical Engineering, Faculty of Engineering, Universiti Malaya, 50603 Kuala Lumpur, Malaysia; [orcid.org/0000-0003-2171-956X](https://orcid.org/0000-0003-2171-956X); Email: [nurinmz@um.edu.my](mailto:nurinmz@um.edu.my)

### Authors

**Muhammad Mujtaba Abbas** – Department of Mechanical Engineering, Faculty of Engineering, Universiti Malaya, 50603 Kuala Lumpur, Malaysia; Department of Mechanical, Mechatronics and Manufacturing Engineering (New Campus), University of Engineering and Technology Lahore, Lahore 54000, Pakistan; [orcid.org/0000-0001-9134-9002](https://orcid.org/0000-0001-9134-9002)

**Syahir Amzar Zulkifli** – Department of Mechanical Engineering, Faculty of Engineering, Universiti Malaya, 50603 Kuala Lumpur, Malaysia

**Md Abul Kalam** – Department of Mechanical Engineering, Faculty of Engineering, Universiti Malaya, 50603 Kuala Lumpur, Malaysia; Centre for Energy Sciences (CFES), Department of Mechanical Engineering, Faculty of Engineering, Universiti Malaya, 50603 Kuala Lumpur, Malaysia

**Muhammad Hazwan Ahmad** – Institute for Advanced Studies, Universiti Malaya, 50603 Kuala Lumpur, Malaysia

**Mohd Nur Ashraf Mohd Yusoff** – Department of Mechanical Engineering, Faculty of Engineering, Universiti Malaya, 50603 Kuala Lumpur, Malaysia

**Mazrina Mazlan** – Institute for Advanced Studies, Universiti Malaya, 50603 Kuala Lumpur, Malaysia

**Wan Mohd Ashri Wan Daud** – Department of Chemical Engineering, Faculty of Engineering, Universiti Malaya, 50603 Kuala Lumpur, Malaysia

Complete contact information is available at:

<https://pubs.acs.org/10.1021/acsomega.1c03073>

## Notes

The authors declare no competing financial interest.

## ACKNOWLEDGMENTS

The authors take the opportunity to thank the Universiti Malaya for the financial support through research grant IIRG008B-2019 under the Universiti Malaya Impact-Oriented Interdisciplinary Research Grant Programme.

## ABBREVIATIONS

B10	Malaysian commercial diesel (90% diesel and 10 palm oil biodiesel)
BP	brake power
BSFC	brake-specific fuel consumption
BT	brake torque
BTE	brake thermal efficiency
CO	carbon monoxide
CO <sub>2</sub>	carbon dioxide
COB	castor oil biodiesel
COF	coefficient of friction
CPME50	50% of cottonseed–palm oil mixture methyl ester in diesel
DEE	diethyl ether
DMC	dimethyl carbonate
FAME	fatty acid methyl ester
GC–MS	gas chromatography and mass spectrometry
HC	hydrocarbons
HFFR	high-frequency reciprocating rig
JB	Jatropha biodiesel
LCFA	long-chain fatty acid
MCFA	medium-chain fatty acid
NO <sub>x</sub>	nitrogen oxide
NP	not present
O <sub>2</sub>	oxygen
OM	optical microscopy
POB	palm oil biodiesel
PP–PE	polypropylene and polyethylene
SCFA	short-chain fatty acid
SF	secondary fuel
SFA	saturated fatty acid
USFA	unsaturated fatty acid
VLCFA	very-long-chain fatty acid
WPO	waste plastic oil
WPO100	100% waste plastic oil
WPO50	50% WPO and 50% POB
WPO60	60% WPO and 40% POB
WPO70	70% WPO and 30% POB
WPO80	80% WPO and 20% POB
WPO90	90% WPO and 10% POB

WSD wear scar diameter

## REFERENCES

- (1) Mujtaba, M.; Cho, H. M.; Masjuki, H.; Kalam, M.; Ong, H.; Gul, M.; Harith, M.; Yusoff, M. Critical review on sesame seed oil and its methyl ester on cold flow and oxidation stability. *Energy Rep.* **2020**, *6*, 40–54.
- (2) Soudagar, M. E. M.; Banapurmath, N. R.; Afzal, A.; Hossain, N.; Abbas, M. M.; Haniiffa, M. A. C. M.; Naik, B.; Ahmed, W.; Nizamuddin, S.; Mubarak, N. M. Study of diesel engine characteristics by adding nanosized zinc oxide and diethyl ether additives in Mahua biodiesel–diesel fuel blend. *Sci. Rep.* **2020**, *10*, No. 15326.
- (3) Dey, S.; Reang, N. M.; Das, P. K.; Deb, M. A comprehensive study on prospects of economy, environment, and efficiency of palm oil biodiesel as a renewable fuel. *J. Cleaner Prod.* **2021**, *286*, No. 124981.
- (4) Zulqarnain; Yusoff, M. H. M.; Ayoub, M.; Jusoh, N.; Abdullah, A. Z. The Challenges of a Biodiesel Implementation Program in Malaysia. *Processes* **2020**, *8*, No. 1244.
- (5) Themelis, N.; Mussche, C. *Energy and Economic Value of Municipal Solid Waste (MSW), Including Non-recycled Plastics (NRP), Currently Landfilled In The Fifty States*; Earth Engineering Center: USA, 2014; pp 1–40.
- (6) Syamsiro, M.; Saptoadi, H.; Norsujanto, T.; Noviasri, P.; Cheng, S.; Alimuddin, Z.; Yoshikawa, K. Fuel Oil Production from Municipal Plastic Wastes in Sequential Pyrolysis and Catalytic Reforming Reactors. *Energy Procedia* **2014**, *47*, 180–188.
- (7) Kaewbuddee, C.; Sukjit, E.; Srisertpol, J.; Maithomklang, S.; Wathakit, K.; Klinkaew, N.; Liplap, P.; Arjharn, W. Evaluation of Waste Plastic Oil-Biodiesel Blends as Alternative Fuels for Diesel Engines. *Energies* **2020**, *13*, No. 2823.
- (8) Singh, R. K.; Ruj, B.; Sadhukhan, A. K.; Gupta, P.; Tigga, V. P. Waste plastic to pyrolytic oil and its utilization in CI engine: Performance analysis and combustion characteristics. *Fuel* **2020**, *262*, No. 116539.
- (9) Sachuthanathan, B.; Reddy, D.; Mahesh, C.; Dineshwar, B. Production of diesel like fuel from municipal solid waste plastics for using in CI engine to study the combustion, performance and emission characteristics. *Int. J. Pure Appl. Math.* **2018**, *119*, 85–96.
- (10) Kalargaris, I.; Tian, G.; Gu, S. Combustion, performance and emission analysis of a DI diesel engine using plastic pyrolysis oil. *Fuel Process. Technol.* **2017**, *157*, 108–115.
- (11) Mangesh, V. L.; Padmanabhan, S.; Tamizhdurai, P.; Ramesh, A. Experimental investigation to identify the type of waste plastic pyrolysis oil suitable for conversion to diesel engine fuel. *J. Cleaner Prod.* **2020**, *246*, No. 119066.
- (12) Khatha, W.; Ekarong, S.; Somkiat, M.; Jiraphon, S. Fuel Properties, Performance and Emission of Alternative Fuel from Pyrolysis of Waste Plastics. *IOP Conf. Ser.: Mater. Sci. Eng.* **2020**, *717*, No. 012001.
- (13) Kumar, R.; Mishra, M.; Singh, S.; Kumar, A. Experimental evaluation of waste plastic oil and its blends on a single cylinder diesel engine. *J. Mech. Sci. Technol.* **2016**, *30*, 4781–4789.
- (14) Singh, T. S.; Rajak, U.; Dasore, A.; Muthukumar, M.; Verma, T. N. Performance and ecological parameters of a diesel engine fueled with diesel and plastic pyrolyzed oil (PPO) at variable working parameters. *Environ. Technol. Innov.* **2021**, *22*, No. 101491.
- (15) Kin, W. E.; Jasmin, A. F. *Plastic: An Undegradable Problem*. License: Creative Commons Attribution CC BY 3.0; Khazanah Research Institute: Kuala Lumpur, 2019.
- (16) Ramesha, D.; Kumara, G. P.; Lalsaheb; Mohammed, A. V.; Mohammad, H. A.; Kasma, M. A. An experimental study on usage of plastic oil and B20 algae biodiesel blend as substitute fuel to diesel engine. *Environ. Sci. Pollut. Res.* **2016**, *23*, 9432–9439.
- (17) Senthilkumar, P.; Sankaranarayanan, G. Effect of Jatropha methyl ester on waste plastic oil fueled DI diesel engine. *J. Energy Inst.* **2016**, *89*, 504–512.

- (18) Lapuerta, M.; García-Contreras, R.; Agudelo, J. R. Lubricity of Ethanol-Biodiesel-Diesel Fuel Blends. *Energy Fuel* **2009**, *24*, 1374–1379.
- (19) Liaquat, A.; Masjuki, H. H.; Kalam, M. A.; Rizwanul Fattah, I. M. Impact of biodiesel blend on injector deposit formation. *Energy* **2014**, *72*, 813–823.
- (20) Awang, M. S. N.; Zulkifli, N. W. M.; Abbass, M. M.; Zulkifli, S. A.; Yusoff, M. N. A. M.; Ahmad, M. H.; Daud, W. M. A. W. Effect of blending local plastic pyrolytic oil with diesel fuel on lubricity. *Jurnal Tribologi* **2020**, *27*, 143–157.
- (21) Damodharan, D.; Sathiyagnanam, A. P.; Rana, D.; Rajesh Kumar, B.; Saravanan, S. Extraction and characterization of waste plastic oil (WPO) with the effect of n-butanol addition on the performance and emissions of a DI diesel engine fueled with WPO/diesel blends. *Energy Convers. Manage.* **2017**, *131*, 117–126.
- (22) Ali, O. M.; Mamat, R.; Abdullah, N. R.; Abdullah, A. A. Analysis of blended fuel properties and engine performance with palm biodiesel–diesel blended fuel. *Renewable Energy* **2016**, *86*, 59–67.
- (23) Razzaq, L.; Mujtaba, M. A.; Soudagar, M. E. M.; Ahmed, W.; Fayaz, H.; Bashir, S.; Fattah, I. M. R.; Ong, H. C.; Shahapurkar, K.; Afzal, A.; Wageh, S.; Al-Ghamdi, A.; Ali, M. S.; El-Seesy, A. I. Engine performance and emission characteristics of palm biodiesel blends with graphene oxide nanoplatelets and dimethyl carbonate additives. *J. Environ. Manage.* **2021**, *282*, No. 111917.
- (24) Tayari, S.; Abedi, R.; Rahi, A. Comparative assessment of engine performance and emissions fueled with three different biodiesel generations. *Renewable Energy* **2020**, *147*, 1058–1069.
- (25) Pinzi, S.; Rounce, P.; Herreros, J. M.; Tsolakis, A.; Pilar Dorado, M. The effect of biodiesel fatty acid composition on combustion and diesel engine exhaust emissions. *Fuel* **2013**, *104*, 170–182.
- (26) Monirul, I. M.; Masjuki, H. H.; Kalam, M. A.; Mosarof, M. H.; Zulkifli, N. W. M.; Teoh, Y. H.; How, H. G. Assessment of performance, emission and combustion characteristics of palm, jatropha and Calophyllum inophyllum biodiesel blends. *Fuel* **2016**, *181*, 985–995.
- (27) Rajkumar, K.; Govindarajan, P. Impact of oxygen enriched combustion on the performance of a single cylinder diesel engine. *Front. Energy* **2011**, *5*, 398–403.
- (28) Ali, O. M. Evaluation of diesel engine performance with high blended diesel-biodiesel fuel from waste cooking oil. *IOP Conf. Ser.: Mater. Sci. Eng.* **2019**, *518*, No. 032054.
- (29) Ruhul, M. A.; Abedin, M. J.; Rahman, S. M. A.; Masjuki, B. H. H.; Alabdulkarem, A.; Kalam, M. A.; Shancita, I. Impact of fatty acid composition and physicochemical properties of Jatropha and Alexandrian laurel biodiesel blends: An analysis of performance and emission characteristics. *J. Cleaner Prod.* **2016**, *133*, 1181–1189.
- (30) Mujtaba, M. A.; Kalam, M. A.; Masjuki, H. H.; Gul, M.; Soudagar, M. E. M.; Ong, H. C.; Ahmed, W.; Atabani, A. E.; Razzaq, L.; Yusoff, M. Comparative study of nanoparticles and alcoholic fuel additives-biodiesel-diesel blend for performance and emission improvements. *Fuel* **2020**, *279*, No. 118434.
- (31) Pan, M.; Qian, W.; Zheng, Z.; Huang, R.; Zhou, X.; Huang, H.; Li, M. The potential of dimethyl carbonate (DMC) as an alternative fuel for compression ignition engines with different EGR rates. *Fuel* **2019**, *257*, No. 115920.
- (32) Hosseini, S. H.; Taghizadeh-Alisaraei, A.; Ghobadian, B.; Abbaszadeh-Mayvan, A. Performance and emission characteristics of a CI engine fuelled with carbon nanotubes and diesel-biodiesel blends. *Renewable Energy* **2017**, *111*, 201–213.
- (33) Heydari-Maloney, K.; Taghizadeh-Alisaraei, A.; Ghobadian, B.; Abbaszadeh-Mayvan, A. Analyzing and evaluation of carbon nanotubes additives to diesel-B2 fuels on performance and emission of diesel engines. *Fuel* **2017**, *196*, 110–123.
- (34) Chauhan, B. S.; Kumar, N.; Cho, H. M. A study on the performance and emission of a diesel engine fueled with Jatropha biodiesel oil and its blends. *Energy* **2012**, *37*, 616–622.
- (35) Imtenan, S.; Masjuki, H. H.; Varman, M.; Arbab, M.; Sajjad, H.; Fattah, I. R.; Abedin, M.; Hasib, A. S. M. Emission and performance improvement analysis of biodiesel-diesel blends with additives. *Procedia Eng.* **2014**, *90*, 472–477.
- (36) Ashok, B.; Nanthagopal, K. 15 - Eco Friendly Biofuels for CI Engine Applications. In *Advances in Eco-Fuels for a Sustainable Environment*; Azad, K., Ed.; Woodhead Publishing, 2019; pp 407–440.
- (37) Gumus, M.; Sayin, C.; Canakci, M. The impact of fuel injection pressure on the exhaust emissions of a direct injection diesel engine fueled with biodiesel–diesel fuel blends. *Fuel* **2012**, *95*, 486–494.
- (38) Khalife, E.; Tabatabaei, M.; Demirbas, A.; Aghbashlo, M. Impacts of additives on performance and emission characteristics of diesel engines during steady state operation. *Prog. Energy Combust. Sci.* **2017**, *59*, 32–78.
- (39) Murcak, A.; Haşimoğlu, C.; Çevik, İ.; Karabektaş, M.; Ergen, G. Effects of ethanol–diesel blends to performance of a DI diesel engine for different injection timings. *Fuel* **2013**, *109*, 582–587.
- (40) Buyukkaya, E. Effects of biodiesel on a DI diesel engine performance, emission and combustion characteristics. *Fuel* **2010**, *89*, 3099–3105.
- (41) Puhan, S.; Saravanan, N.; Nagarajan, G.; Vedaraman, N. Effect of biodiesel unsaturated fatty acid on combustion characteristics of a DI compression ignition engine. *Biomass Bioenergy* **2010**, *34*, 1079–1088.
- (42) Sharon, H.; Jai Shiva Ram, P.; Jenis Fernando, K.; Murali, S.; Muthusamy, R. Fueling a stationary direct injection diesel engine with diesel-used palm oil–butanol blends – An experimental study. *Energy Convers. Manage.* **2013**, *73*, 95–105.
- (43) Mosarof, M. H.; Kalam, M. A.; Masjuki, H. H.; Alabdulkarem, A.; Habibullah, M.; Arslan, A.; Monirul, I. M. Assessment of friction and wear characteristics of Calophyllum inophyllum and palm biodiesel. *Ind. Crop. Prod.* **2016**, *83*, 470–483.
- (44) Nabi, M. N.; Rahman, M. M.; Islam, M. A.; Hossain, F. M.; Brooks, P.; Rowlands, W. N.; Tulloch, J.; Ristovski, Z. D.; Brown, R. J. Fuel characterisation, engine performance, combustion and exhaust emissions with a new renewable Licella biofuel. *Energy Convers. Manage.* **2015**, *96*, 588–598.
- (45) Sanjid, A.; Masjuki, H. H.; Kalam, M. A.; Rahman, S. M. A.; Abedin, M. J.; Reza, M. I.; Sajjad, H. Experimental Investigation of Palm-jatropha Combined Blend Properties, Performance, Exhaust Emission and Noise in an Unmodified Diesel Engine. *Procedia Eng.* **2014**, *90*, 397–402.
- (46) Ong, H. C.; Masjuki, H. H.; Mahlia, T. M. I.; Silitonga, A. S.; Chong, W. T.; Yusaf, T. Engine performance and emissions using Jatropha curcas, Ceiba pentandra and Calophyllum inophyllum biodiesel in a CI diesel engine. *Energy* **2014**, *69*, 427–445.
- (47) Wu, G.; Ge, J. C.; Choi, N. J. A Comprehensive Review of the Application Characteristics of Biodiesel Blends in Diesel Engines. *Appl. Sci.* **2020**, *10*, No. 8015.
- (48) Habibullah, M.; Masjuki, H. H.; Kalam, M.; Fattah, I. R.; Ashraful, A.; Mobarak, H. Biodiesel production and performance evaluation of coconut, palm and their combined blend with diesel in a single-cylinder diesel engine. *Energy Convers. Manage.* **2014**, *87*, 250–257.
- (49) Knothe, G. Dependence of biodiesel fuel properties on the structure of fatty acid alkyl esters. *Fuel Process. Technol.* **2005**, *86*, 1059–1070.
- (50) An, H.; Yang, W. M.; Chou, S. K.; Chua, K. J. Combustion and emissions characteristics of diesel engine fueled by biodiesel at partial load conditions. *Appl. Energy* **2012**, *99*, 363–371.
- (51) Gharehghani, A.; Mirsalim, M.; Hosseini, R. Effects of waste fish oil biodiesel on diesel engine combustion characteristics and emission. *Renewable Energy* **2017**, *101*, 930–936.
- (52) Özener, O.; Yükksek, L.; Ergeng, A. T.; Özkan, M. Effects of soybean biodiesel on a DI diesel engine performance, emission and combustion characteristics. *Fuel* **2014**, *115*, 875–883.
- (53) Arunkumar, M.; Kannan, M.; Murali, G. Experimental studies on engine performance and emission characteristics using castor biodiesel as fuel in CI engine. *Renewable Energy* **2019**, *131*, 737–744.

(54) Perumal, V.; Ilangkumaran, M. Experimental analysis of engine performance, combustion and emission using pongamia biodiesel as fuel in CI engine. *Energy* **2017**, *129*, 228–236.

(55) Uyumaz, A. Combustion, performance and emission characteristics of a DI diesel engine fueled with mustard oil biodiesel fuel blends at different engine loads. *Fuel* **2018**, *212*, 256–267.

(56) Sivakrishna, T.; Madhu, D.; Sivakumar, K. The effect of palm biodiesel fuel on the performance of automotive four stroke diesel engine. *IOP Conf. Ser.: Mater. Sci. Eng.* **2019**, *574*, No. 012015.

(57) Mujtaba, M. A.; Muk Cho, H.; Masjuki, H. H.; Kalam, M. A.; Farooq, M.; Soudagar, M. E. M.; Gul, M.; Ahmed, W.; Afzal, A.; Bashir, S.; Raju, V. D.; Yaqoob, H.; Syahir, A. Z. Effect of alcoholic and nano-particles additives on tribological properties of diesel–palm–sesame–biodiesel blends. *Energy Rep.* **2021**, *7*, 1162–1171.

(58) Gul, M.; Zulkifli, N.; Masjuki, H.; Kalam, M.; Mujtaba, M.; Harith, M.; Syahir, A.; Ahmed, W.; Farooq, A. B. Effect of TMP-based-cottonseed oil-biolubricant blends on tribological behavior of cylinder liner-piston ring combinations. *Fuel* **2020**, *278*, No. 118242.

(59) Fazal, M. A.; Haseeb, A. S. M. A.; Masjuki, H. H. Investigation of friction and wear characteristics of palm biodiesel. *Energy Convers. Manage.* **2013**, *67*, 251–256.

(60) Pehan, S.; Jerman, M. S.; Kegl, M.; Kegl, B. Biodiesel influence on tribology characteristics of a diesel engine. *Fuel* **2009**, *88*, 970–979.

(61) Mujtaba, M. A.; Kalam, M. A.; Masjuki, H. H.; Soudagar, M. E. M.; Khan, H. M.; Fayaz, H.; Farooq, M.; Gul, M.; Ahmed, W.; Ahmad, M.; Munir, M.; Yaqoob, H.; Samuel, O. D.; Razzaq, L. Effect of palm-sesame biodiesel fuels with alcoholic and nanoparticle additives on tribological characteristics of lubricating oil by four ball tribo-tester. *Alex. Eng. J.* **2021**, *60*, 4537–4546.

(62) Masjuki, H.; Maleque, M. Investigation of the anti-wear characteristics of palm oil methyl ester using a four-ball tribometer test. *Wear* **1997**, *206*, 179–186.

(63) Kumar, A. N.; Srinivas Kishore, P.; Raju, K.; Kasianantham, N.; Ashok, B. Engine parameter optimization of palm oil biodiesel as alternate fuel in CI engine. *Environ. Sci. Pollut. Res.* **2019**, *26*, 6652–6676.

(64) Jamshaid, M.; Masjuki, H. H.; Kalam, M. A.; Mohd Zulkifli, N. W.; Ahmed, A.; Zulfattah, Z. M. Effect of Fatty Acid Methyl Ester on Fuel-Injector Wear Characteristics. *J. Biobased Mater. Bioenergy* **2020**, *14*, 327–339.

(65) Mujtaba, M. A.; Masjuki, H. H.; Kalam, M. A.; Noor, F.; Farooq, M.; Ong, H. C.; Gul, M.; Soudagar, M. E. M.; Bashir, S.; Rizwanul Fattah, I. M.; Razzaq, L. Effect of Additivized Biodiesel Blends on Diesel Engine Performance, Emission, Tribological Characteristics, and Lubricant Tribology. *Energies* **2020**, *13*, 3375.

(66) Juwono, H.; Fauziah, L.; Uyun, I. Q.; Alfian, R.; Suprpto; Ni'mah, Y. L.; Ulfan, I. In *Catalytic Conversion of Al-MCM-41-Ceramic on Hydrocarbon (C8–C12) Liquid Fuel Synthesis from Polypropylene Plastic Waste*, AIP Conference Proceedings; AIP Publishing LLC: 2018; 020080.

(67) Mujtaba, M. A.; Masjuki, H. H.; Kalam, M. A.; Noor, F.; Farooq, M.; Ong, H. C.; Gul, M.; Soudagar, M. E.; Baig, S.; Rizwanul Fattah, I. M.; Razzaq, L. Effect of Additivized Biodiesel Blends on Diesel Engine Performance, Emission, Tribological Characteristics, and Lubricant Tribology. *Energies* **2020**, *13*, No. 3375.